

**UNCLASSIFIED**

---

---

**AD 400 524**

---

*Reproduced  
by the*

**ARMED SERVICES TECHNICAL INFORMATION AGENCY  
ARLINGTON HALL STATION  
ARLINGTON 12, VIRGINIA**



---

---

**UNCLASSIFIED**

---

NOTICE: When government or other drawings, specifications or other data are used for any purpose other than in connection with a definitely related government procurement operation, the U. S. Government thereby incurs no responsibility, nor any obligation whatsoever; and the fact that the Government may have formulated, furnished, or in any way supplied the said drawings, specifications, or other data is not to be regarded by implication or otherwise as in any manner licensing the holder or any other person or corporation, or conveying any rights or permission to manufacture, use or sell any patented invention that may in any way be related thereto.

63-3-1

FTD-TT- 62-860

CATALOGED BY ASTIA  
AS AD NO. 400524

# TRANSLATION

MEASUREMENT OF LINEAR ACCELERATIONS

By

N. P. Rayevskiy and M. I. Subbotin

## FOREIGN TECHNOLOGY DIVISION

AIR FORCE SYSTEMS COMMAND

WRIGHT-PATTERSON AIR FORCE BASE

OHIO



# UNEDITED ROUGH DRAFT TRANSLATION

MEASUREMENT OF LINEAR ACCELERATIONS

BY: N. P. Rayevskiy and M. I. Subbotin

English Pages: 74

S/5702

THIS TRANSLATION IS A RENDITION OF THE ORIGINAL FOREIGN TEXT WITHOUT ANY ANALYTICAL OR EDITORIAL COMMENT. STATEMENTS OR THEORIES ADVOCATED OR IMPLIED ARE THOSE OF THE SOURCE AND DO NOT NECESSARILY REFLECT THE POSITION OR OPINION OF THE FOREIGN TECHNOLOGY DIVISION.

PREPARED BY:

TRANSLATION SERVICES BRANCH  
FOREIGN TECHNOLOGY DIVISION  
WP-AFB, OHIO.

Akademiya Nauk SSSR

IZMERENIYE LINEYNYKH USKORENIY

Izdatel'stvo Akademii Nauk SSSR  
Moskva 1961

Pages: 1-62

FTD-TT-62-860/1+2

TABLE OF CONTENTS

Introduction . . . . .	1 •
1. Measurement of Maximum Values of the Acceleration	4
2. Apparatus for Measuring Maximum Accelerations . .	8
3. Fundamentals of the Theory of Accelerometers with Inertial Elements . . . . .	13
4. Design of Accelerometers . . . . .	21
5. Experimental Determination of Accelerometer Con- stants . . . . .	30
6. Sensors for Linear Accelerations with Inertial Elements . . . . .	36
7. Measurement of Impact Accelerations . . . . .	49
8. Sensors for Measurement of Impact Acceleration .	54
9. Calibration of Impact Accelerometers . . . . .	61
References . . . . .	68

## INTRODUCTION

When confronted with the dynamic design of machine mechanisms, it is necessary to consider the inertial loads which act on the components of these machine mechanisms.

The magnitude of the inertial forces is dependent on the individual components; therefore, calculation of the inertial forces is linked to determination or calculation of the accelerations of the components of the mechanism. In the majority of cases, however, the magnitude and the change in the accelerations, particularly during an irregular pattern of machine movement where the accelerations acquire increased values and complex forms of change, can only be determined experimentally.

The characteristic nature of acceleration measurements consists in the fact that accelerations are extremely varied and that accelerometers\* have a comparatively small range of measurement magnitudes. In addition, the most important characteristic of an acceleration is not its magnitude, but its rise time. The longer the period of acceleration increase, the easier it is to develop an accelerometer for it. It is extremely difficult to build an accelerometer for accelerations with small magnitudes and at the same time for those with extremely short periods of acceleration increase, because the sensitivity of an accelerometer is an inverse function of its natural frequency. Short-term accelerations, however, are rarely small and, generally, small accelerations increase slowly. The limits of measurable accelerations are extremely large: starting with the smallest and slowest reckoned in

fractions of a  $g$  for a whole and for tenths of a second and extending to a thousand  $g$ 's which increase over a period of from 250 to 500 microseconds. Thus, the mean linear acceleration of an automobile which is propelled in 15 seconds from a velocity of 0 to 50 km/hour will be approximately 0.14  $g$ . The acceleration of the cutting tool of a planing machine is 0.8  $g$  in the forward direction and 0.83  $g$  in the reverse direction.

When testing machines, accelerations measurable in tens of  $g$ 's are encountered considerably more frequently and the upper limit of nonimpact accelerations should be regarded as from 100 to 150  $g$ .

The larger accelerations occur on impact. Thus, the maximum acceleration on impact of a steel rod falling face first onto an anvil from a height of 5 cm is approximately 1500  $g$ . When impact velocities are large, accelerations may arise which have magnitudes measured in tens of thousands of  $g$ 's.

In practice, one of two problems generally arises when measuring accelerations: to measure the maximum value of an acceleration and to measure the acceleration as a function of time. In the first case, the accelerations often have significant magnitudes and their determination is dependent on measurement of forces. In the latter case, the accelerations are not extremely large and their determination is associated with investigation of the movements of the components of the mechanism.

In conformity with this, accelerometers are divided into two groups. The large number of maximum-range accelerometers belong to the first group. Accelerometers for recording a process in time must be included in the second group.

Descriptions of accelerometers based on the use of various methods of measurement may be found in the literature relating to meas-

urement techniques. There are mechanical, optical, hydraulic, electrical, and other accelerometers which measure accelerations over various frequency and acceleration ranges. Among the electrical accelerometers are slide-wire, inductive, semi-conductive, electrodynamic, and other accelerometers. In operation, electrical linear acceleration sensors with wire-wound strain-gage pickups and piezoceramic sensors made of barium titanate are considered the most highly perfected and simplest accelerometers with respect to design. Sections 1.6 to 8 were written by N.P. Rayevskiy and sections sections 2 to 5 and 9 by M.I. Subbotin.

What has been said about sensors in regard to their design, determination of their characteristics, and parameter selection pertains, in large measure, to all accelerometers regardless of their operating principle.

## 1. MEASUREMENT OF MAXIMUM VALUES OF THE ACCELERATION

There are many problems associated with measurement of maximum values of the acceleration. For example, there is the determination of accelerations and forces during forging, stamping, and bending, as well as the determination of the accelerations on impact of the components of the mechanisms, etc.

The necessity of building maximum accelerometers was also governed by the fact that recently, in industry, we have begun to apply methods of checking final products by shock with a certain acceleration value which is difficult to determine, and the investigators are often uncertain as to whether their tests correspond to industrial requirements.

The most primitive method of determining acceleration is to observe the behavior of sand particles on a vibrating surface. If a particle of sand is driven from a surface by vibration, the acceleration associated with the vibration exceeds one  $g$ .

The first maximum accelerometer was proposed by Academician B. B. Golitsyn.

A diagram showing the principle of one of his accelerometers, which is a parallelepiped with sides  $b$  and  $h$ , is shown in Fig. 1. Under a constant acceleration  $a$ , the point at which the parallelepiped begins to turn about edge  $o$  occurs under the condition

$$\frac{Q}{g} a \frac{h}{2} = Q \frac{b}{2}, \text{ or } a = \frac{b}{h} g.$$

Thus, the magnitude of an acceleration measured by this instru-

ment is dependent upon the ratio  $b/h$ .

Another instrument due to Academician B.B. Golitsyn consisted of a weight  $P$  suspended by threads from point  $A$  (Fig. 2). With an acceleration magnitude  $a$  equal to  $g \tan \alpha$ , the electrical contact between the weight and the bearing is broken and, in this way, the maximum

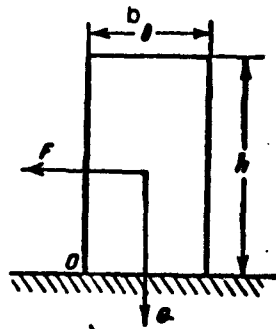


Fig. 1. Maximum accelerometer due to Academician B.B. Golitsyn.

value of the acceleration in question is recorded. Varying the angle  $\alpha$ , we can measure the various limiting values of the acceleration. Many different maximum accelerometers have been constructed on this principle of contact breaking. A set of such accelerometers adjusted to various limiting acceleration values and connected to a device which records the number of electrical contact breaks, serves to characterize the process being measured by registering the number of ac-

celerations of different magnitudes over a determined period of time or for a given path segment (for example, the jolting of an automobile traveling over various roads).

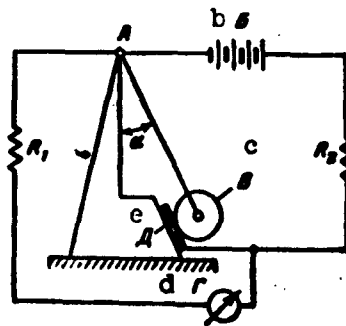


Fig. 2. Maximum accelerometer due to Academician B.B. Golitsyn.

Other designs for maximum accelerometers have been based on various methods of measuring the inertial force of a given constant mass. Figure 3 shows diagrams of these designs.

The inertial force may be measured by breaking the thread or wire.

In certain cases, this method has proved to be unsuitable, since the thread which is attached by one end to a body cannot transmit the velocity of the body to the weight to which the other end is attached; therefore, the loading conditions of

the thread will not agree with the test conditions. In these cases, the thread is replaced with a rod of ebonite or other brittle material with a notch, the dimensions of which determine the breaking forces.

The inertial force may also be measured by the distortion of the vertex of a wax cone or the change in the diameter of a red-copper

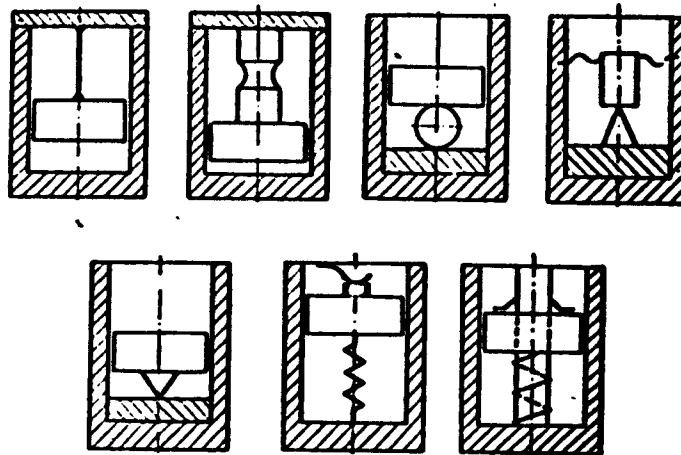


Fig. 3. Diagrams of maximum accelerometers.

sphere, which are compressed by a weight (crushing method), or by measuring the impressions left by a cone or sphere of a hard material (diamond, steel) on steel, copper, or lead strips having known mechanical properties (scleroscope method). Sometimes, methods involving contact-making or recording the magnitude of spring compression under the action of a weight by using a special catch, etc., are applied in place of contact breaking.

These methods are not characterized by high accuracy and are approximate.

In every case, the magnitude of an acceleration will be

$$a = \frac{P}{Q} g \text{ m/sec}^2$$

or  $a = P/Q$  in units of  $g$  if the measured force is equal to  $P$  and the constant mass of the weight  $m = Q/g$ .

Existing designs of maximum accelerometers have, more often than other types, circuits with contact breakers. Figure 4 shows one of these designs.

In the absence of acceleration ( $a = 0$ ), the depressing force of the arm AK which is exerted by the weight  $mg$  and by the compression of the spring B will be  $Q_0$  on contact. Where there is a dynamic effect on the apparatus, the force changes by an amount

$$\frac{mal}{L} = \frac{Ia}{IL} = \frac{Ia}{I}$$

and will be equal to

$$Q = Q_0 - \frac{Ia}{I}$$

where  $I$  is the moment of inertia of the movable portion of the apparatus relative to point A.

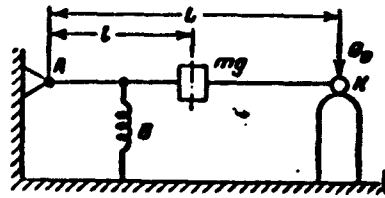


Fig. 4. Maximum accelerometer with breaking contact.

The contact is broken when  $Q = 0$ ; whence,  $Q_0 = Ia/IL$ . Thus, contact breaking occurs at an acceleration

$$a = Q_0 \frac{I}{I} = cQ_0$$

where  $c = Ll/I$  is a constant of the equipment which is dependent upon the position of the weight, the length of the arm AK, and the moment of inertia  $I$ .

On varying the force of the spring compression and the position of the weight, we may adjust the sensor to measure various values of the acceleration.

One of the latest designs of a maximum accelerometer has been described in the foreign technical literature. A total of 8 bracket arms with a small weight at the end are bent by screws driven into the weight. Contact between these components can be broken at the moment when the inertial force exerted on the mass of the beam exceeds the

initial tension on the beam. Each beam is connected electrically to a neon lamp whose beam is reflected onto photopaper or film driven by a timing mechanism. When contact is made, a straight line is recorded on the paper and when contact is broken, the line is discontinued; this indicates an acceleration having a magnitude which corresponds to the tension on the beam. The number of broken lines and their spacings determine the nature and form of the acceleration being measured. A separately installed electric bulb which flashes a determined number of times per second records the time.

There is also a description of a maximum accelerometer in which a permanent magnet holds several steel spheres in its field of attraction. The attractive force on these spheres varies because they are separated from the magnet by nonmagnetic insertion pieces of different thicknesses. Under the influence of an acceleration, the spheres which are attracted by a smaller force break away from the magnet; this indicates the limits between which the measured acceleration lies.

The maximum accelerometers under consideration measure small as regards magnitude (10-15 g), and slowly increasing (hundredths of a second) accelerations more accurately. Impacts are measured with large errors which reach 15 to 30%.

## 2. APPARATUS FOR MEASURING MAXIMUM ACCELERATIONS

A special apparatus for measuring maximum accelerations is more universal and enables us to obtain higher accuracy. It measures the maximum acceleration for individual and periodic impacts, as well as for vibrations, by operating in conjunction with a piezoaccelerometer and is actually an impulse voltmeter. The indicator in it serves as a needle-type microammeter. Its reading is retained for a period of 10 seconds after measurement.

A diagram of the apparatus is shown in Fig. 5. The first stage -

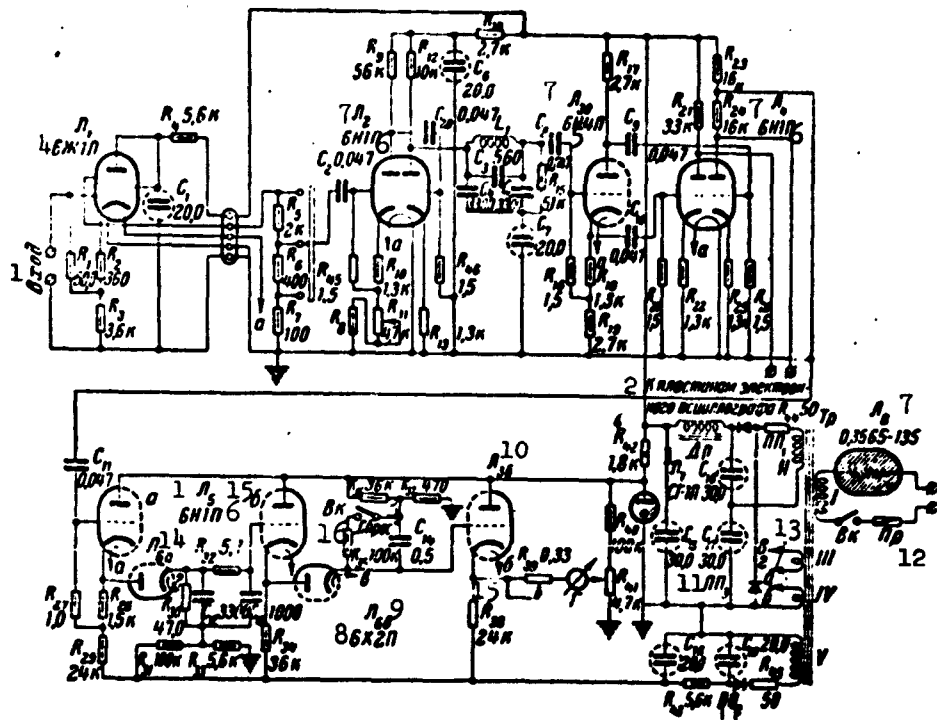


Fig. 5. Basic circuit of instrument used to measure maximum accelerations. 1) Input; 2) to electronic oscillograph plates; 3) breaker; 4) 6Zh1p; 5) 6N4P; 6) 6N1P; 7) L; 8) 6Kh2p; 9) L<sub>6b</sub>; 10) L<sub>3b</sub>; 11) PP<sub>3</sub>; 12) Pr; 13) G; 14) L<sub>6a</sub>; 15)  $\underline{b}$ ; 16) "throw."

a pullout cathode follower — is generally used for circuits with piezo-sensors. A signal from this stage is relayed to a three-stage voltage divider having a separation coefficient of 1:5 for each stage. A two-stage voltage amplifier follows. By varying the resistance R<sub>11</sub> in the cathode circuit of one of the tubes, we can vary the amplification by

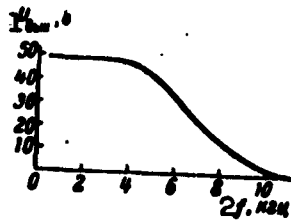


Fig. 6. Frequency characteristic of apparatus. 1)  $U_{vykh}$ , volts; 2)  $f$ , kcps.

approximately  $\pm 10\%$ ; this is necessary to adjust the range of the apparatus. A low-pass filter following the amplifier cuts out the high-frequency vibrations which arise in the accelerometer on impact and which distort the form of the signal being measured. The transmission band of the filter is determined by the conditions of the measurements and can be limited by a frequency of  $2/t_0$  ( $t_0$  is the duration of the measurable impulse). In the apparatus under consideration, the break begins at 5 kcps (Fig. 6). Such a band permits transmission of an almost undistorted sinusoidal impulse with a period of 400 microseconds. Impulses of approximately this form and duration

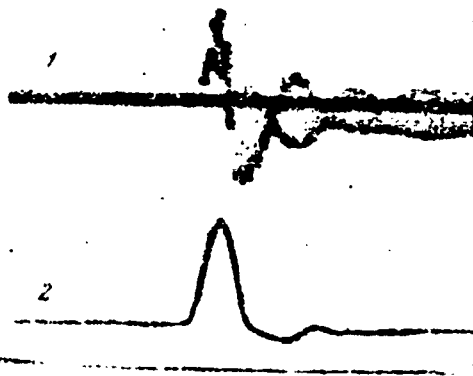


Fig. 7. Influence of transmission band on recording. 1) 12 kcps band; 2) 6 kcps band.

arise during calibration of the accelerometers on the ballistic pendulum described below. Shorter impulses are scarcely encountered in measurement practice.

The necessity of a filter is illustrated by Fig. 7. A phase inverter and a push-pull final stage follow the filter. A signal may be fed from the output of the last stage to an electronic oscillograph for examination or recording of the impulse being measured. The maximum undistorted voltage at the output is 55 amplitude volts.

The signal from the final stage of the amplifier is fed to a voltmeter. The circuit of the voltmeter is similar to that of an impulse attenuator described in the literature [34]. The circuit oper-

ates in the following manner. A positive voltage impulse, entering the grid of the cathode follower  $L_{5a}$  and proceeding through diode  $L_{6a}$ , charges condenser  $C_{12}$ , which has a charging time constant of several microseconds, to its peak value. At the same time,  $C_{13}$  begins to receive a charge, but considerably more slowly, since its charge passes through the large resistor  $R_{32}$ . After the effect of the impulse has

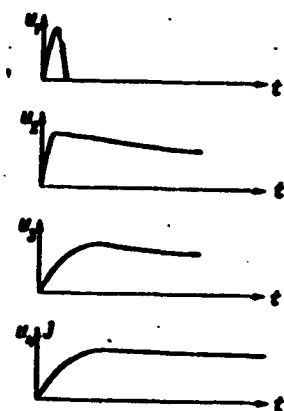


Fig. 8. Time Curves of voltages in circuit of instrument.  $U_1$ ) Input pulse on grid  $L_{5a}$ ;  $U_2$ ) on capacitance  $C_{12}$ ;  $U_3$ ) on capacitance  $C_{13}$ ;  $U_4$ ) on capacitance  $C_{14}$ ; J) Current through indicator.

ceased,  $C_{12}$  discharges slowly through  $R_{30}$  in such a manner that its voltage drops below 1% when  $C_{13}$  is fully charged.

The voltage on  $C_{13}$  is transmitted to the grid of the succeeding cathode follower  $L_{5b}$ , which charges the large capacitance  $C_{14}$  through diode  $L_6$ . As a result of the low front steepness of the impulse acting on the  $L_{5b}$  grid, the tube is not overloaded and  $C_{13}$  is not discharged by its grid current.

When the toggle switch Bk is open, the discharge of  $C_{14}$  occurs as a result of leakage and the grid current of the tube  $L_{3b}$ . Generally, in this situation, an electrometric tube is employed, but this greatly complicates and increases the cost of the circuit. In the apparatus, we used a double 6N4P triode having a smaller grid current than any of the tubes generally used.

The final stage of the instrument is a voltmeter across a bridge circuit; its null point is balanced with the aid of  $R_{41}$ . The time curves of the voltages in the circuit are shown in Fig. 8.

A negative voltage is supplied to the cathodes of  $L_{5a}$  and  $L_{5b}$  to increase the dynamic range. A supporting voltage of approximately

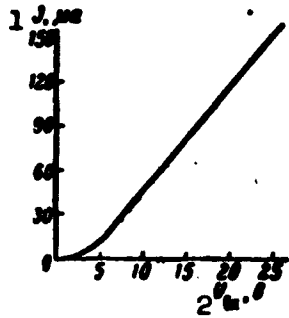


Fig. 9. Calibration curve of apparatus voltmeter.  
 1) J, microamps;  
 2)  $U_{vkh}$ , volts.

0.5 volts is supplied to  $C_{14}$ ; this eliminates the initial charge on  $C_{14}$  and the slipping of the null point which this causes and which occurs after the toggle switch Ek is opened ("throwing").

The anode voltage of the voltmeter is stabilized with a stabilatron. The filament of  $L_6$  is supplied from a well-insulated glowing winding. After installation, the  $L_{3b}$  panel is treated with a solution of plexiglas in dichloroethane to reduce surface leakage.

The apparatus has the following characteristics:

- Acceleration ranges . . . . . 0-20, 0-100 and 0-500 g
- Measurement error . . . . . 10%
- Sensitivity of  
 accelerometer . . . . . 3 millivolts/g
- Number of tubes . . . . . 8
- Feed . . . . . off a 220 volt line
- Input . . . . . 65 watts
- Dimensions . . . . . 220 X 10 X 180 mm<sup>3</sup>
- Weight . . . . . 4.5 kg.

Calibration of the apparatus is performed twice: first with electrical impulses of accurately measured amplitude, and then on a ballistic pendulum in series with the accelerometer. A calibration curve of the voltmeter is shown in Fig. 9.

It is necessary to regulate the accelerometer so that it produces a positive impulse on impact.

The ranges of the apparatus may be easily varied in both directions. The basic purpose of the apparatus is to operate in impact and

vibration endurance tests.

### 3. FUNDAMENTALS OF THE THEORY OF ACCELEROMETERS WITH INERTIAL ELEMENTS

In simplest form, an apparatus of the inertial type is an inert mass suspended from a spring with a damper (Fig. 10), i.e., a vibrating system with one degree of freedom. This implies the following: 1) the mass of the spring is negligibly small and the spring deforms on vibration as a single body; 2) only the damper creates a resistance to motion; 3) the motion of the inert mass is in only one direction.

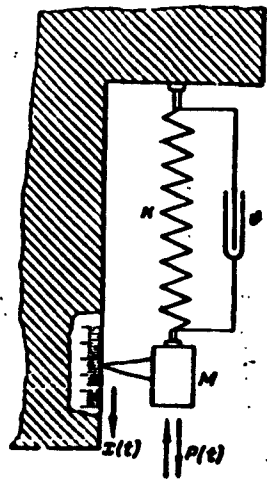


Fig. 10. Diagram of accelerometer with inertial element.

Moreover, it is generally assumed that when the spring is deformed, Hooke's law is strictly observed and the resistance is proportional to the velocity of the inert mass.

In actual practice, in the general case, all the above conditions are not satisfied; therefore, the system under consideration is ideal. In many cases, however, the system is a good approximation to reality and investigation of it leads easily to a final result; therefore, we shall study precisely this system. More accurate results will be elaborated as needed.

It should be noted that the presence of parasitic (unaccounted for) degrees of freedom has little effect on the operation of an accelerometer at low frequencies. A much stronger influence is exerted by the non-linearity of the elastic and resistance forces: this non-linearity must be kept to a minimum, as far as possible.

Sometimes, an inertial apparatus with several degrees of freedom is designed deliberately for special purposes [4], or, in other words, the system shown in Fig. 10 becomes more complicated.

Many studies of the applied theory of vibrations, for example, [12, 16] and [30], have been devoted to apparatus of the inertial type; here, therefore, we shall limit ourselves to a summary exposition of certain determinations and conclusions from this theory.

The equation describing the operation of the apparatus by the system shown in Fig. 10 is

$$M\ddot{x} + F_v + F_e + P(t),$$

where  $M$  is the magnitude of the inert mass,  $F_u$  is the elastic force,  $F_s$  is the resistance,  $P(t)$  is the external force, and  $x$  is the displacement of the inert mass from the equilibrium position.

If the conditions of linearity

$$F_v = -\epsilon \dot{x}; \quad F_e = -kx$$

(the minus sign indicates the direction of action of the forces) are satisfied, the equation presented earlier may be written in the form

$$\ddot{x} + 2\epsilon \dot{x} + \omega_0^2 x = a(t), \quad (1)$$

where

$$2\epsilon = \frac{b}{M}, \quad \omega_0^2 = \frac{k}{M}, \quad a(t) = \frac{P(t)}{M}$$

The constants  $\epsilon$  and  $\omega_0$  fully characterize the apparatus and therefore bear the special designations: "damping constant" and "natural frequency," respectively. Frequently, another quantity - the damping coefficient  $D = \epsilon/\omega_0$  - is considered in place of  $\epsilon$ .

The two quantities  $\omega_0$  and  $D$  are united under the designation "apparatus constants." The natural frequency  $\omega_0$  is expressed in rad/sec and is greater than the quantities of the same designation measured in cycles per second by a factor of  $2\pi$ .  $D$  is a dimensionless quantity generally smaller than unity.

Where there are no external forces present, the motion of the inert mass obeys the law of damped vibrations

$$x(t) = Ae^{-\epsilon t} \sin(\sqrt{\omega_0^2 - \epsilon^2} t + \varphi). \quad (2)$$

This motion is termed "the natural vibrations of the apparatus." The constants  $A$  and  $\psi$  are determined by the initial conditions.

Motion under the action of external forces is called "forced." Under a constant external force  $P_0$ , the displacement of the inert mass will also have a constant magnitude:

$$x_0 = \frac{1}{\omega_0^2} \frac{P_0}{M} = \frac{1}{\omega_0^2} a_0 \quad (3)$$

Since  $a_0$  is the acceleration acting on the inert mass,  $x_0$  will give the magnitude of this acceleration on the  $1/\omega_0^2$  scale (units of length per unit of acceleration).

Therefore, the apparatus is also an accelerometer whose sensitivity is determined by the coefficient  $1/\omega_0^2$ . The acceleration due to gravity,  $g = 981 \text{ cm/sec}^2$ , is very frequently taken as the unit of acceleration.

If, however, at the time  $t = 0$ , a harmonic force begins to act on the apparatus so that  $a(t) = a_0 \sin \omega t$ , then

$$x(t) = Ae^{-\alpha t} \sin(\sqrt{\omega_0^2 - \alpha^2} t + \psi) + Ua_0 \sin(\omega t + \varphi) \quad (4)$$

where  $U$  and  $\varphi$  are functions of the vibration frequency  $\omega$

$$U(\omega) = \frac{1}{\sqrt{(\omega_0^2 - \omega^2)^2 + 4\alpha^2\omega^2}} \quad (5)$$

$$\varphi = -\arctan \frac{2\alpha\omega}{\omega_0^2 - \omega^2}$$

$U$  is termed "the frequency" (more precisely speaking, the amplitude-frequency) characteristic of the apparatus, while  $\varphi$  is the phase characteristic. The significance of  $U$  and  $\varphi$  is explained by the fact that, after damping of the natural vibrations, the motion of the inert mass will also be harmonic with the amplitude  $Ua_0$  and with the displacement with respect to phase  $\varphi$ . Curves of  $U(\omega)$  and  $\varphi(\omega)$  for various values of  $D$  are shown in Figs. 11 and 12.

It is easy to see that at a sufficiently low vibration frequency

$$\omega \ll \omega_0$$

$$U \approx \frac{1}{\omega} = \text{const } \varphi \approx 0, \quad (6)$$

i. e., the apparatus will record accelerations on the same  $1/\omega_0^2$  scale. In other words, it will act as accelerometer.

If, however, Conditions (6) are not satisfied, all the acting accelerations can, nevertheless, be determined from Formula (5). But this is possible only in the case of an external harmonic force. In all other cases of variable force, the motion of the inert mass will not reproduce the accelerations due to the frequency and phase distortions induced by the apparatus.

A condition involving the absence of distortions can be formulated in the following manner.  $a(t)$  can almost always be represented in the form of a Fourier series or integral [16]. As a rule, the amplitudes of the spectrum components decrease with frequency. If the natural frequency  $\omega_0$  of an accelerometer is so high that conditions (6) are satisfied for all spectrum components which have more or less significant amplitudes, there will be no distortions. For the most part, the condition  $\varphi \approx 0$  may replace the less rigid one. It is simple to prove that where there is a phase displacement proportional to the frequency,  $x(t)$  differs from  $a(t)$  only by a constant displacement in time which, when required, may be accounted for without difficulty. Therefore, the criterion for the absence of distortions is

$$U \approx \text{const}, \varphi \approx (\text{const}) \omega. \quad (6a)$$

The frequency range in which these approximate equalities are valid is the operating range of the accelerometer.

A guarantee of the fulfillment of Conditions (6a) with a given accuracy in a given frequency range is also a problem in accelerometer design.

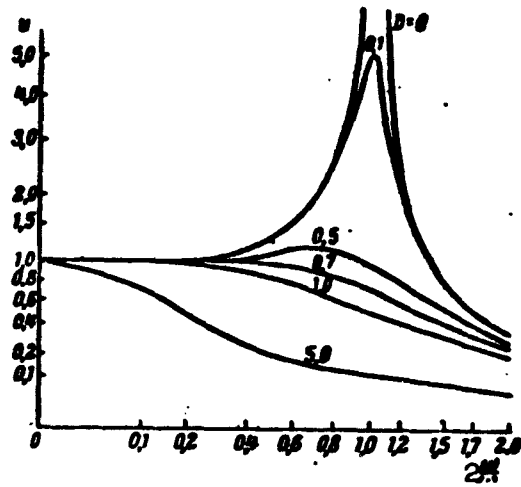


Fig. 11. Amplitude-frequency characteristic of accelerometer for various values of D.

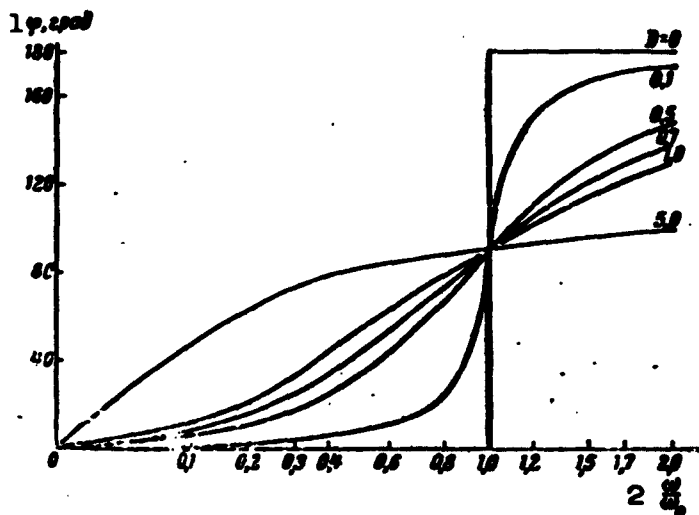


Fig. 12. Phase-frequency characteristic of accelerometer for various values of D. 1)  $\varphi$ , degrees.

It is obvious that the requirements of high sensitivity and a broad operating range are contradictory: the broader the range, the lower will be the sensitivity. Therefore, we must find a compromise solution and if there is no provision for sensitivity, it is possible

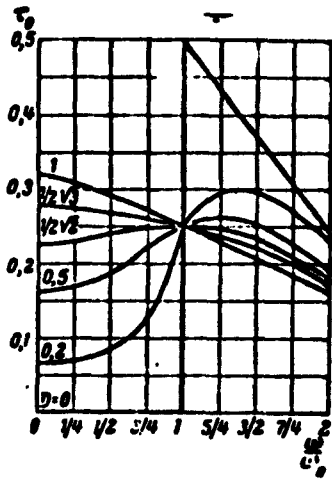


Fig. 13. Dependence of time displacement in accelerometer on frequency.

to select a smaller  $\omega_0$ . For this purpose, we must know, at least approximately, the frequency range of the acceleration being investigated. Therefore, occasionally we have to select the natural frequency of an accelerometer by the method of successive approximation. It is desirable that it be at least double the the highest frequency in the spectrum of the process.

Subsequently, we must select an optimum value of the damping coefficient  $D$ . It is apparent from the frequency characteristics (Figs. 11 and 12) that when  $D = 0.67$ , the effective range of the accelerometer will extend from 0 to  $0.8 \omega_0$  (the frequency characteristic in this range is almost constant; the rise in the vicinity of  $0.6 \omega_0$  is extremely small). The phase charac-

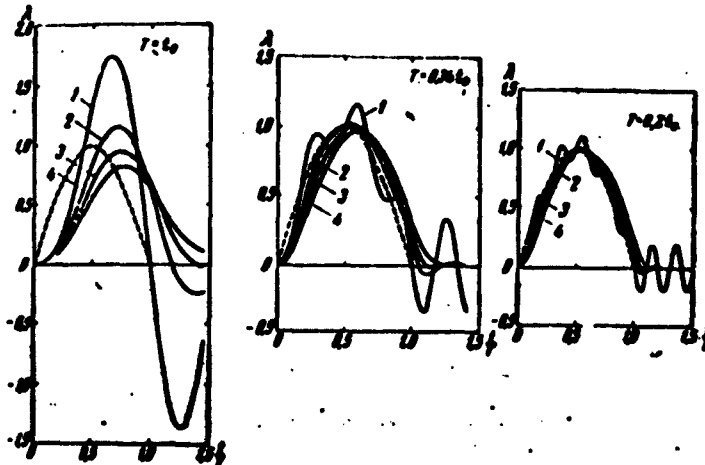


Fig. 14. Reproduction of sinusoidal impulse by accelerometer. 1)  $D = 0$ ; 2)  $D = 0.4$ ; 3)  $D = 0.7$ ; 4)  $D = 1.0$ .

teristic in this same range, however, deviates significantly from the linear. Therefore, the effective range will be narrower for the same

value of  $D$  (up to  $0.4 \omega_0$ ).

It is possible to determine the effective range in such a way that the time displacements of all the harmonic components, the frequencies of which are within the range, are almost identical. Obviously, if the phase displacement is  $\varphi$  at a frequency  $\omega$ , the time displacement is

$$\tau = \frac{\varphi}{\omega}. \quad (7)$$

It is convenient to consider the relative displacement

$$\tau_0 = \frac{\tau}{T_0} = \frac{\varphi}{2\pi/\omega_0} = \frac{\varphi}{T_0} \quad (7a)$$

where  $T_0$  is the period of free vibration of the accelerometer in the absence of damping.

A curve taken from [38] illustrates what has been stated above (Fig. 13). We may conclude from Fig. 13 that when  $D = 0.77$ ,  $\tau_0 = 0.25$  for  $0 < \omega < \omega_0$ . Therefore, the form distortions due to phase displacement will not be present. But here, the frequency distortions will cause the effective range to contract by approximately  $0.5 \omega_0$ . Thus, there are two possibilities:

1. If phase distortions do not play a major role in the nature of the measurement (for example, when determining the range of the process) we may take  $D = 0.67$ ; in this case, the error in the amplitude will be less than 1% for  $0 < \omega < 0.5 \omega_0$ , but the phase characteristic will be linear within  $4^\circ$  in the same frequency range [21].

2. If, however, minimum phase distortions are significant, it is necessary to assume the value 0.77 for  $D$ . The deviation of the phase characteristic from a straight line is  $0.5^\circ$  less in the same  $0 < \omega < 0.5 \omega_0$  range. The frequency characteristic will have a slope of 4% for a frequency of  $0.4 \omega_0$  and 7% for a frequency of  $0.5 \omega_0$ .

In the majority of cases, these data permit the accurate selec-

tion of values for the accelerometer constants. In a few cases, accelerometers must be selected otherwise to measure impact accelerations. It is a question here of individual impulses or of periodic impulses with small recurrence frequencies. Generally, these last for a short time - from a few milliseconds to tenths of a millisecond, and there are sharp fronts and breaks in their form.

In this case, the natural frequency of the accelerometer must be

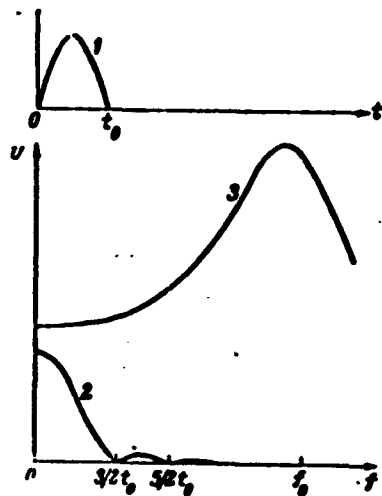


Fig. 15. Selection of natural frequency for impulse measurements. 1) Measured impulse; 2) impulse range; 3) frequency characteristic of accelerometer.

selected as high as possible for the following reasons. It is necessary to have an accelerometer with a broad frequency range for accurate reproduction of sharp fronts. But in accelerometers with high natural frequencies, we cannot succeed in creating maximum damping: too large resisting forces are required. Therefore, on impact, natural vibrations arise which distort the recording. They will cease rapidly if the period of the natural vibrations is significantly smaller than the duration of the impulse and the distortions will be less noticeable (Fig. 14). Finally, when

the natural frequency is increased, the sensitivity will decrease, but here a compromise is necessary.

In selecting the natural frequency, we must proceed from the anticipated range of the impulse to be measured. An impulse of rectangular form is rarely encountered during measurement. The form of the impact pulse is more frequently nearly triangular or sinusoidal. With such a form, the impulse range extends approximately to a frequency equal to  $2/t_0$  (in cycles per second), where  $t_0$  is the dura-

tion of the impulse. The higher-frequency components have extremely small amplitudes. Therefore, the natural frequency  $\omega_0$  should be equal to (8-10)  $2\pi/t_0$  (Fig. 15).

When measuring the impulses of other forms, the requirements for the natural frequency of an accelerometer vary. More detailed information relating to this is given by Yu. I. Iorish [16].

It is impossible to regard all high-frequency accelerometers as systems with one degree of freedom. The presence of many degrees of freedom implies the existence of a large number of natural frequencies. It is, of course, most important to know the lowest of these frequencies which we will denote as  $\omega_0$ .

#### 4. DESIGN OF ACCELEROMETERS

In this section are considered design problems for the simplest type of low-frequency accelerometer with a given natural frequency, the design of a damper (generally liquid) and the question of sensitivity in accelerometers with strain-gage pickups.

Design of accelerometer with a given natural frequency  $\omega_0$ . Here we shall consider an accelerometer of the simplest design as shown in Fig. 16a in which the elastic element is a flat spring operating under a deflection. Accelerometers with elastic elements of other forms do not permit use of strain-gage pickups and therefore will not be considered.

In designing an accelerometer, it is expedient to consider it as a system with an infinite number of degrees of freedom, since the mass of the elastic element is comparable to or greater than the inert mass. The design of complex set-ups is rather laborious [1], but nomograms [26] have been compiled for the design of the simplest accelerometers (Fig. 16). One of these nomograms which refers to the structural design shown in Fig. 16a is located at the end of the book (Fig.

48).

The natural frequency (here and in what follows this will refer to the natural frequency  $f_0$  in cycles per second which is equal to

$\omega_0/2\pi$ ) of the bending vibrations of the spring is computed by the formula

$$f_0 = 0.046 c \frac{h}{l^2} \lambda_1^2 \quad (8)$$

where  $h$  is the thickness of the spring,  $l$  is its length,  $c = \sqrt{E/\rho}$  is the propagation rate of the longitudinal waves in the spring material and  $\lambda_1$  is the least root of the so-called frequency equation [1].

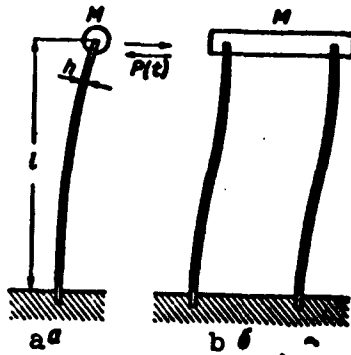


Fig. 16. Accelerometers with flat springs. a) With one spring; b) with two springs.

In the case cited above, the frequency equation has the form

$$1 + \cos \lambda ch \lambda = \frac{M}{m} \lambda (\sin \lambda ch \lambda - \cos \lambda sh \lambda), \quad (9)$$

where  $M/m$  is the ratio of the inert mass and the mass of the spring.

The nomogram constructed from Equations (8) and (9) makes it possible to design accelerometers with a frequency of 10-500 cps with an elastic element prepared from steel, Dural, brass, bronze or Mi-carta. The length and thickness of the spring are taken as initial data in addition to the natural frequency and the material of the spring. The spring width  $b$  and the size of the inert mass  $M$  are found from the nomogram. Naturally, it is possible to produce a design from any other combination of the four given initial data. It is also possible to calculate the frequency of an instrument which has already been constructed.

The use of the nomogram may be explained by the simple design in Fig. 49. Let it be required to design an accelerometer for the data:  $f_0 = 50$  cps, spring material - bronze,  $l = 40$  mm and  $h = 0.5$  mm. Let

us construct a straight line through points  $\underline{l} = 40$  and  $\underline{l} = 5$  on the corresponding scales intersecting the left-hand scale B where we mark the point of intersection. Let us construct a straight line through this point of intersection and the point  $f = 50$  to intersect the left-hand vertical of the diagram. From the point of intersection, we must now draw a horizontal straight line to cross the "bronze" curve, and then along the vertical to the straight "bronze" line and again horizontally to the right-hand edge of the diagram, where it is necessary to mark one point of intersection.

Then it is required to construct a straight line through points  $\underline{l}' = 40$  and  $h' = 0.5$  on the  $\underline{l}'$  and  $h'$  scales. Let us connect the point of intersection of this line with the right-hand scale A with the point of intersection on the right-hand edge of the diagram; this gives a point of intersection on the C scale. Now, let us select any given pair of values  $M$  and  $\underline{v}$  lying on the straight line which passes through the point obtained on the C scale. For example, we may take  $M = 5$  grams and  $b = 0.5$  mm.

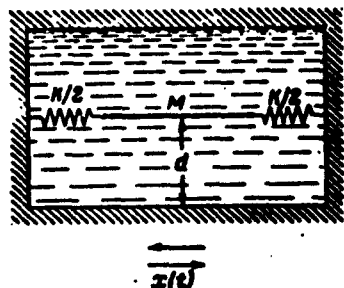


Fig. 17. Simplified diagram of accelerometer with liquid damping.

The accuracy of the design is highly dependent upon the physical properties of the materials employed. In general, the discrepancy between calculated and experimental results did not exceed 5-10%, increasing with an increase in  $f_0$  to 200-300 cps and greater.

The elastic stresses in the spring, for the most part, cannot be calculated, since the deflection of the spring in the accelerometer is usually negligible, and the recording unit has provision for sensitivity.

Design of damper in accelerometer. Of all the means of damping in

an accelerometer the most used is fluid damping, since electromagnetic or pneumatic damping does not make it possible to attain the large resistance forces required for high natural frequencies.

Where there is damping by a viscous liquid, the casing of the accelerometer is filled with the liquid. The interaction of the inert mass and the spring with the liquid in the presence of vibration will create a resisting force. In the general case, it is difficult to determine this force, because it is impossible to calculate it from the proportional velocity of the weight; this is sometimes simply assumed.

A viscous liquid is described by the Navier-Stokes equations, while the force which the liquid exerts on a body moving through it is found by solution of these equations under the corresponding boundary conditions. The proportionality of the resisting force and the velocity is observed only where there is movement of a solid body through an infinite liquid with a constant velocity, and then only under the condition that the Reynolds number is small [19]. For the case of the vibratory motion of a body in a viscous liquid, the effective force consists of two components, one of which is proportional to the velocity of the body while the other is proportional to its acceleration. The first component is dependent on the viscosity and is the resisting force "in pure form"; the second component, however, arises because the moving body transmits a certain impulse to the liquid and some part of it appears as a vibration. This effect may be interpreted as an increase in the mass of the body to the so-called "associated mass of the liquid." This effect is independent of the viscosity and of the dimensions of the given surface of the body. In other words, it is not connected with adhesion, but with the displacement of a certain portion of the liquid. The coefficients in the formulas for both forces are functions of the vibration frequency.

If the volume of the liquid, however, is finite, the phenomenon becomes considerably more complicated. The phenomenon can be described mathematically by solving the nonlinear partial differential equations under variable boundary conditions. This problem can hardly be solved by the usual methods. But the equations can be solved for one simplified model [27]. Let us reduce the solution to an abbreviated form. A simulation of an accelerometer with liquid damping is shown in Fig. 17. A flat plate with mass  $M$  and surface area  $S$  on both sides can vibrate in its own plane between two walls parallel to it. The front face of the plate is obviously assumed to be infinitely small. The walls and plate are connected by an elastic tie and the space between the walls is filled with a viscous liquid.

Considering the free vibration of this simulated model, we can draw the conclusion that when certain determined conditions are fulfilled, the movement during a sufficiently small period of time will obey the function

$$x(t) = x_0 e^{-\epsilon t} \cos \sqrt{\omega_0^2 - \epsilon^2} t; \quad (10)$$

Here  $\omega_0'$  and  $\epsilon$  are constant magnitudes

$$\omega_0' = \frac{\omega_0}{\left(1 + \frac{m_1}{2M}\right)^{1/2}}, \quad \text{and } \epsilon = \frac{\rho \delta}{2M \left(1 + \frac{m_1}{2M}\right)}, \quad (11)$$

where  $\omega_0$  is the natural frequency of the simulated model empty of liquid,  $\underline{d}$  is the clearance between the plate and walls,  $\rho$  is the density of the liquid,  $m_1$  is the mass of the liquid in the space, and  $\nu$  is the kinematic viscosity of the liquid.

As is apparent, the natural frequency is decreased subsequent to filling the apparatus with the liquid, but where there are small clearances, this decrease is insignificant: even if  $m_1/M = 0.3$ , the natural frequency changes only 5%. On the other hand, to obtain a large damping coefficient  $\epsilon/\omega_0'$ , the clearance  $\underline{d}$  must be small, and it is precisely this which decreases the change in the natural frequency.

Thus, the simulated model under consideration describes an accelerometer with a constant  $\omega_0'$  and  $\epsilon$ .

The solution of the problem of forced vibrations of the model shows that if the inequality

$$\frac{\omega^2}{\nu} < 1, \quad (12)$$

is satisfied, the characteristics of the model will be given by Formulas (5) with the substitution of  $\omega_0$  for  $\omega_0'$ . If we assume  $d \approx 0.1$  cm and  $\nu \approx 10$  stokes (these are far from being limiting values), it follows from (12) that

$$\omega < 1000, \text{ i. e., } f = \frac{\omega}{2\pi} < 150 \text{ cps.}$$

In what follows is given a comparison of an accelerometer built taking into account the conclusions stated above with an accelerometer of ordinary design.

Electromagnetic damping is used only in vibrometers. It has indisputable advantages — a strictly linear relationship of the damping force to the velocity, the feasibility of more accurate regulation of the damping coefficient, and a minor dependence on temperature. But the available magnetic materials do not enable us to attain large damping forces, and the dimensions and weight of the accelerometer increase.

In order to evaluate the feasibility of electromagnetic damping, let us show a design for the simplest construction — a short circuited ring in an axially symmetrical magnetic field (Fig. 18). Designs of other types of electromagnetic dampers are considerably more complex and less accurate [3].

When the ring vibrates along its axis, the force

$$F_c = \frac{2\pi r B^2 A}{2\pi \rho_0} 2\pi r B \dot{z} = \frac{2\pi r^2 A}{\rho_0} B^2 \dot{z} = \frac{\nu^2 B^2}{2\pi} \dot{z} \cdot 10^{-9}$$

acts on the ring, where  $B$  is the induction in gauss,  $\rho_0$  is the specific resistance of the ring material in ohms mm<sup>2</sup>/m, and  $v'$  is the volume of that portion of the ring in the magnetic field. Hence,

$$D = \frac{F_c}{2M\omega_0^2} = \frac{v'B^2}{2(M_1 + M_2)\rho_0\omega_0^2} \cdot 10^{-8} \quad (13)$$

( $M = M_1 + M_2$ , where  $M_2$  is the mass of the ring). In order to increase  $D$  where  $B$ ,  $\rho_0$  and  $\omega_0$  are constants, it is necessary to decrease  $M_1$ .

At the limit, the mass of the inertial element is equal to the mass of the ring; this means that

$$D_{max} = \frac{v'B^2}{2M\rho_0\omega_0^2} \cdot 10^{-8} = \frac{v'B^2}{2\alpha\rho_0\omega_0^2} \cdot 10^{-8} = \frac{\alpha B^2}{2\rho_0\omega_0^2} \cdot 10^{-8} \quad (13a)$$

where  $\delta$  is the density of the ring material,  $v$  is the volume of the ring and  $\alpha = v'/v < 1$ . As is apparent, it is desirable to make the ring of a material with a high  $(\rho_0\delta)^{-1}$  value. For constantan this is 0.24; manganin, 0.31; silver, 6.0; copper, 6.5; aluminum, 13.5.

If it is necessary to take  $D = 0.7$  when  $B = 5 \cdot 10^3$ , the ring is of aluminum, and  $\alpha = 0.35$ , then

$$f_0 < \frac{1}{2\pi} \frac{\alpha B^2}{2\rho_0\omega_0} \cdot 10^{-8} \approx 130 \text{ cps.}$$

This maximum value of  $f_0$  should be recognized as slightly on the high side, since it is difficult to obtain an induction of 5000 gauss in a clearance which is not extremely small. Thus, if the apparatus must operate over a broad temperature range, it is necessary to take measures to stabilize the apparatus constants. The temperature coefficients of resistance for copper and aluminum are approximately 0.004; therefore, for a temperature change of 50°C, the resistance changes by 20%. If, however, constantan or manganin is used,  $f_{0 \text{ max}}$  will decrease by a factor of ten.

This calculation explains why electromagnetic damping is practically never used in accelerometers.

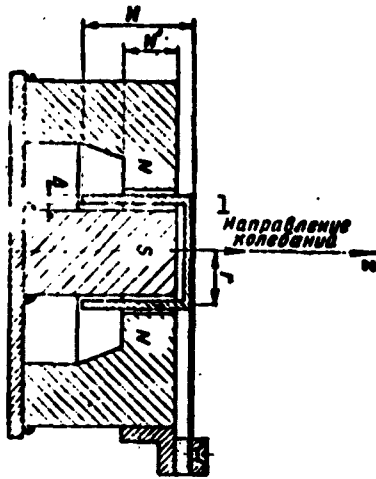


Fig. 18. Diagram of magnetic damping. 1) Direction of vibrations.

Where liquid damping is employed, it is desirable to use highly viscous silicon-organic liquids with a reduced temperature coefficient of viscosity. Several of these liquids are described in the literature [2].

Sensitivity of accelerometers with strain-gage pickups. This problem, which can be important in the design of accelerometers, has been examined in detail in the literature [29].

An accelerometer with strain-gage pickups is shown schematically in Fig.

19. If we assume the nomenclature in Formula (8) with the additions apparent from Fig. 19, we obtain the expression

$$\xi = \xi_0 \frac{M \Omega_1^2}{m f_0^2} \left( 1 - \frac{2x_s^2 + a}{2l} \right). \quad (15)$$

for the sensitivity to accelerations, where  $\xi_0$  is a constant magnitude.

It is apparent from this expression that it is advantageous to take a natural frequency  $f_0$  as low as measurement conditions will allow. However, in contrast to Formula (3), the relationship here is inversely proportional. It is advantageous to make the elastic element from a material with a low  $c$ . Values of the magnitude of  $c^{-1}$  for certain materials in relative units are as follows: steel and Dural - 1.0, bronze - 1.4, and brass and Micarta - 1.5.

Of course, when selecting the material and dimensions of the elastic element, it is necessary to take care that in operation the deformation does not go beyond the proportionality limit, and to take

into account the temperature relationship of the elastic properties.

The sensitivity is also dependent upon the magnitude  $M\lambda_1^2/m$ , which increases with increasing  $M/m$ , as we have shown in the curve in Fig.

20.

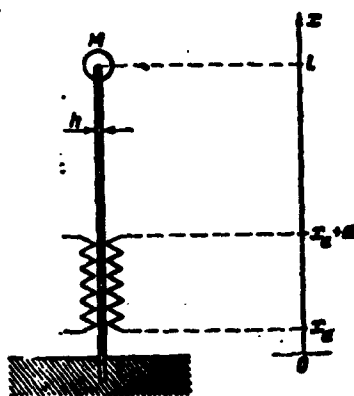


Fig. 19. Diagram of accelerometer with strain-gage pickups.

It follows from Eq. (15) that it is desirable to glue the strain-gage pickups as near as possible to the end of the spring that is fastened to the casing and that the base of the sensor should be as small as possible.

If we have an accelerometer such as is shown in Fig. 16b, we can double the sensitivity by gluing four sensors to the

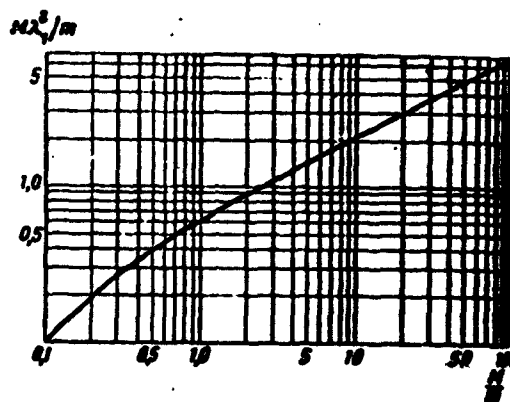


Fig. 20. Curve used to calculate sensitivity of accelerometer with strain-gage pickups.

spring (symmetrically about middle of the spring) and connecting them into a full bridge circuit.

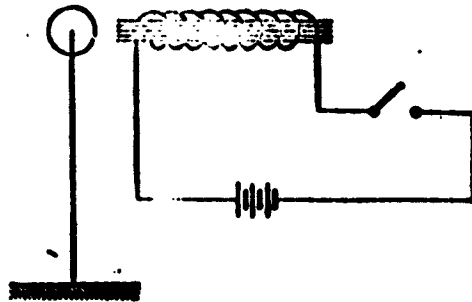


Fig. 21. Circuit for excitation of natural vibrations.

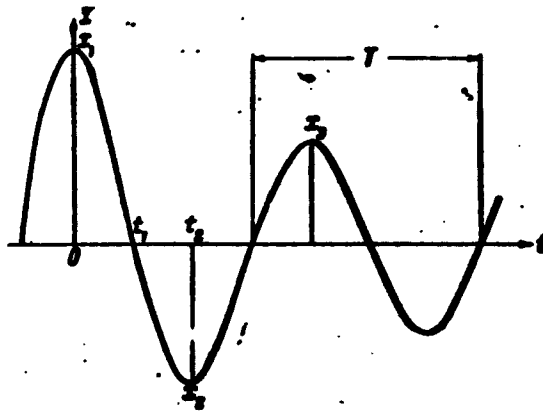


Fig. 22. Natural vibrations of an accelerometer.

##### 5. EXPERIMENTAL DETERMINATION OF ACCELEROMETER CONSTANTS

Such a determination is carried out after an accelerometer has been built, to check its design.

In certain cases the design is extremely inaccurate or is simply not feasible; then, the values of the constants can only be obtained by experiment.

As a rule, the constants of an apparatus are determined by an oscillogram of its natural vibrations which have been excited by any given method. If the inertial element is made of steel, it is convenient to use the scheme shown, Fig. 21, in which we may set, by choice,

either the initial displacement or the initial velocity.

The method generally adopted is described by Iorish and Rayevskiy [16] and [22]. It consists in determining  $\omega_0$  and D from the equations

$$\omega_0 = \frac{2}{T} \sqrt{x^2 + \ln^2 \frac{x_1}{x_2}} \quad (16)$$

$$D = \frac{\ln \frac{x_1}{x_2}}{\sqrt{x^2 + \ln^2 \frac{x_1}{x_2}}} \quad (16a)$$

The designations T,  $x_1$  and  $x_2$  may be understood from Fig. 22. Formulas (16) and (16a) are valid only in that case where the resisting force is proportional to the velocity. The criterion for this is the constant relation between any two successive maximum deviations in one direction. Curves of Formulas (16) and (16a) are shown in Fig. 23 and 24.

However, this method in which the amplitude relationships come into play will give sufficient accuracy only when D is small.  $D \approx 0.7$ ,  $x_2/x_1$  will be approximately 1/20 and may hardly be measured with sufficient accuracy. Therefore, sometimes we proceed as follows: decreasing the damping (for example, by not filling the accelerometer casing with a liquid), the vibration "period" T' is determined from the oscillogram. If the damping coefficient is of the order of 0.1, then

$$T' = T_0 = \frac{2\pi}{\omega_0} \quad (17)$$

with a greater accuracy.

Subsequently, the nominal damping is established and the vibration "period" T" is found. But

$$T' = \frac{T_0}{\sqrt{1-D^2}}$$

Consequently,

$$D = \sqrt{1 - \left(\frac{T'}{T_0}\right)^2} \quad (17a)$$

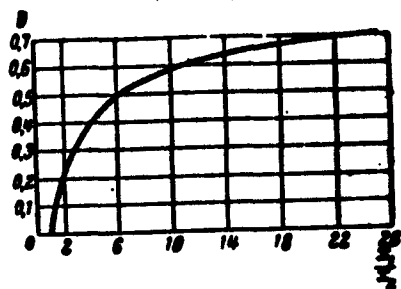


Fig. 23. Curve for determination of D.

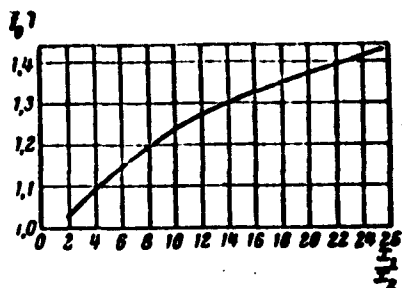


Fig. 24. Curve for determination of  $f_0$ .

Zakharov [13] proposed that in determination of D the apparatus be filled with some low-viscosity liquid. This helps to reduce the error

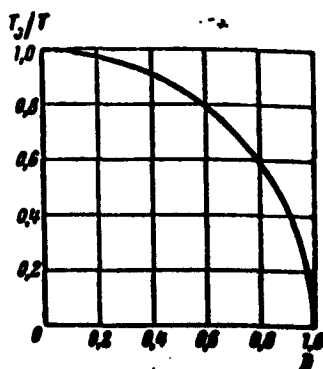


Fig. 25. Dependence of  $T_0/T$  on D.

accuracy of the reading.

Using the relationships

We may use the curve of Fig. 25 which is plotted on the basis of this formula. It is only necessary to note that, in the case of liquid damping, this method may produce a significant error, since the reduction in the natural frequency due to the "associated mass of the liquid" is not taken into consideration. Let us illustrate this with an example: for one of the accelerometers, it was found from Formulas (16) and (16a) that

$$\omega_0 = 2\pi \cdot 43 \text{ cps}; D = 0.1,$$

$$\text{and since } T' = 0.020 \text{ sec and } T'' = 0.023 \text{ sec}$$

$$\omega = 2\pi \cdot 50 \text{ cps}; D = 0.5$$

on the basis of Formulas (17) and (17a).

error if the densities of this liquid and the damping liquid are close to each other.

The determination of the constants is facilitated where the method based on the measurement of time relationships during natural vibrations is employed [28]. This method requires a considerably stepped-up recording rate. It is expedient to excite vibrations with short impulses; this increases the ac-

$$t_1 = \frac{1}{\omega_0 \sqrt{1-D^2}} \arctan \frac{\sqrt{1-D^2}}{D}; \quad t_2 = \frac{\pi}{\omega_0 \sqrt{1-D^2}}$$

we find

$$\omega_0 = \frac{\pi}{t_2} \operatorname{cosec} \frac{\pi t_1}{t_2}; \quad D = \cos \frac{\pi t_1}{t_2}. \quad (18)$$

When computing with these formulas, it is important to construct the null line properly and to take into account the thickness of the line on the oscillogram.

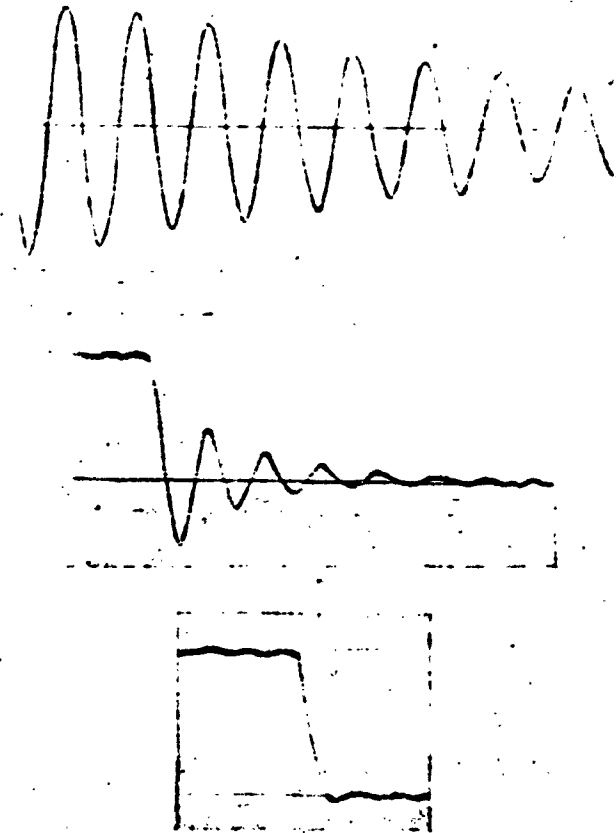


Fig. 26. Oscillogram of natural vibrations for various values of  $D$ .

Figure 26 shows the oscillograms of the natural vibrations of an accelerometer with a gradual increase in the damping coefficient.

It is possible to propose still another means of determining the

constants under conditions of harmonic vibration. To carry this out, it is necessary to have a "vibrostand" which produces vibrations of good form and sufficient amplitude over a range of frequencies close to the calculated natural frequency of the accelerometer, the frequency meter, and the phase meter. Let us first determine the natural

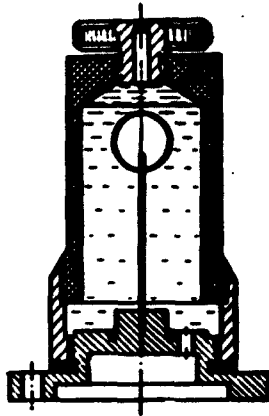


Fig. 27. Accelerometer with spherical weight.

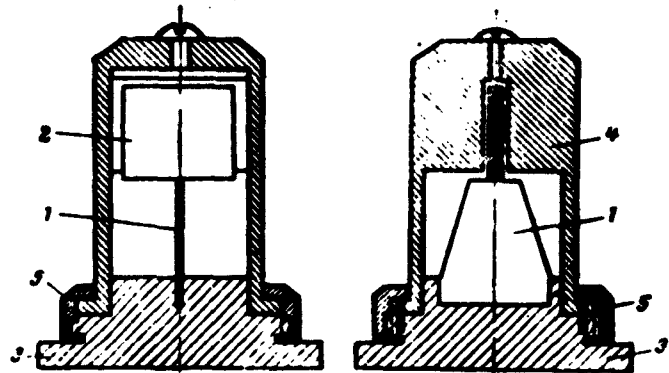


Fig. 28. "Flat" accelerometer. 1) Elastic element; 2) inert mass; 3) base; 4) casing; 5) cover nut.

frequency  $f_0$ : this is that frequency at which the phase displacement between the vibrations of the stand and of the inert mass of the apparatus is  $\pi/2$ . For greater accuracy, we must note the two frequencies at which the phase displacement is  $\pi/2 - \beta$  and  $\pi/2 + \beta$ , respectively ( $\beta$  is a small angle) and take their geometric mean. Then  $D$  is formed from the phase displacement for any given frequency  $f$  that is not too close to  $f_0$ .

$$D = \frac{1 - (f/f_0)^2}{2f/f_0} \tan \varphi.$$

In the absence of a phase meter, the phase displacement may be determined from an oscillogram of the forced vibrations, but this is less satisfactory.

The coincidence of the values  $\omega_0$  and  $D$  calculated by the method described above serves as a guarantee of the good quality of the ac-

celerometer.

Data relating to the reduction of  $\omega_0$  where one of the accelerometers is dampened by a liquid has been cited above. This was an accelerometer of the type shown in Fig. 27. Its damping coefficient was selected by varying the viscosity of the liquid by purely empirical means. In contrast to this, a "flat" accelerometer (Fig. 28) was designed in advance. Its design data:  $f_0 = 50$  cps and  $D = 0.7$ . It was established from the natural vibrations that  $f_0 = 47$  cps in air,  $f_0 = 46$  cps in the casing filled with silicone, and  $D = 0.6$ . The determination of  $D$  from the phase characteristic gave a value of 0.6-0.65. Several accelerometers were built on the basis of this principle. Using liquids with viscosities of from 10 to 20 stokes, it is easy to obtain the required value for  $D$ , as low as 1, even where the natural frequency is 500 cps, and perhaps at even higher frequencies.

In the most favorable cases, the determination of the constants, in particular  $D$ , was carried out with an accuracy to 5%. Therefore, when designing, there is no point in proceeding from the values of the constants calculated with an accuracy to three decimal places as is sometimes done.

As for high-frequency accelerometers, however, only the lowest natural frequency  $f_0$  is usually determined. The natural vibrations are excited by a sudden impact on the casing. In this case, for piezoccelerometers with elastic elements operating under a compressive or shearing stress, the lowest natural frequency determined by the elastic element and the inert mass generally exceeds tens of kilocycles per second. It is not this frequency, but the lowest natural frequencies of the casing that are observed on the oscillogram. Therefore, it is not necessary to compute the natural frequency of the piezoaccelerometer. In measuring, it is necessary to pay particular attention to

the attachment of the accelerometer to the object of measurement.

#### 6. SENSORS FOR LINEAR ACCELERATIONS WITH INERTIAL ELEMENTS

A basically simple design of sensor used to measure linear accelerations consists of a vertically positioned elastic cantilever beam embedded in a base and with a weight fastened to the free upper end. When the base of the sensor is set in motion with the acceleration to be measured, the inertial force of the mass of the weight will bend the cantilever beam. Under determined conditions, this bending will be

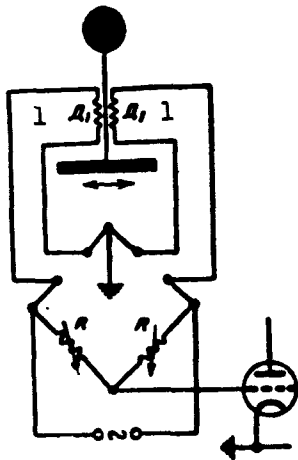


Fig. 29. Electric circuit of linear acceleration sensor.  
1)  $D_1$ .

proportional to the acceleration applied to the base. The bending of the beam can be measured with the use of wire strain-gage pickups which are placed on the two sides of the beam. This beam is placed in a casing filled with a damping fluid of a determined viscosity. From the strain-gage pickups there are leads which are connected to the terminals situated on the casing of the sensor. In the electric circuit, these strain-gage pickups comprise two arms of the measuring bridge (Fig. 29) which is connected to the

input of an amplifier.

Being at the same temperature, the sensors attached to the beam are heat compensators which eliminate the influence of temperature variations.

For a straight cantilever beam, the greatest bending moment and the greatest deformations are at the base of the beam and the strain-gage pickups to be glued on the beam should be situated at the fastened end. For beams with small dimensions, strain-gage pickups with small bases are required for attachment.

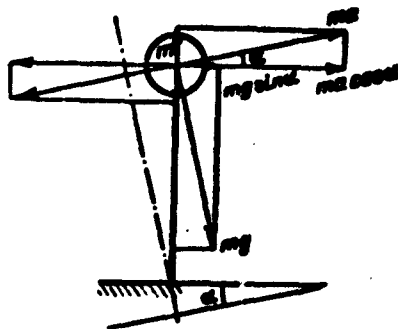


Fig. 30. Influence of incorrect setting of accelerometer.

In order that the relative deformation be the same along the length of the beam, it must have the form of a beam of equal resistance. For such a beam, the moment of resistance along the beam must decrease proportionally with a change in the bending moment. The radius of curvature of such a beam is

$$r = \frac{EI}{M},$$

i. e., the beam will bend in the form of an arc of a circle, and its deflection will be one and one-half times greater than that of a straight beam. The relative deformation

$$\frac{\Delta l}{l} = \frac{M}{EW},$$

where  $W$  is the moment of resistance at the base.

The deformation will be the same over the entire length of the beam and of the strain-gage pickups; therefore, the pickups may be arranged along the entire length of the beam.

A linear acceleration sensor may have a different sensitivity as a function of the natural frequency. The lower the natural frequency, the greater the sensitivity. The sensitivity of a sensor to acceleration may be expressed by different values: by the voltage at the bridge output (millivolts/g), by the relative change in resistance  $(\Delta R/R)/g$ , and by the relative deformation  $(\Delta l/l)/g$  referred to unit of acceleration.

Since measured accelerations are usually recorded on an oscillogram, it is convenient to determine the sensitivity of a sensor in mm/g - millimeters of the oscillogram's ordinate corresponding to

one  $g$ , or in  $n$   $g/mm$  - the number of  $g$ 's per millimeter of the ordinate.

The sensitivity of a linear acceleration sensor, together with the frequency of the natural vibrations, is the fundamental characteristic of the sensor.

When the sensor is rotated  $90^\circ$  from the vertical, its reading will correspond to 1  $g$ . The rotation should be accomplished with sufficient accuracy, since sensors with low natural frequencies already begin to respond to rotations of from 1 to  $2^\circ$ ; this may be noted on the oscillogram. Obviously, an inaccurate setting of the sensor at the time of calibration or measurement may lead to errors.

Let us assume that we are to measure linear accelerations with an inaccurately mounted sensor having a deviation in the direction of the acceleration to be measured (Fig. 30). The spring of the sensor will bend under the force  $ma \cos \alpha$ , the inertial force component of which is to be measured.

In addition to this, the component of the force of gravity  $mg \sin \alpha$  will also bend the spring. Consequently, the spring will bend under the influence of the force

$$P = ma \cos \alpha + mg \sin \alpha.$$

If the acceleration to be measured is small and is approximately equal to  $g$ , then

$$P \approx mg(\sin \alpha + \cos \alpha).$$

For small angles,  $\sin \alpha$  is close to zero and  $\cos \alpha$  is close to unity; therefore, their sum is also close to unity but somewhat greater.

In cases where the motion is in the opposite direction, the sum will be somewhat smaller than unity.

$$P \approx mg(\cos \alpha - \sin \alpha)$$

On recording a harmonic vibration, this produces a displacement of the

null line from its mean value, although the sum of the amplitudes will be recorded without the error arising from the deviation.

It follows from this that in calibration and measurement, the amplitudes of the vibrations should be determined from the sum of the upward and downward deviations; this can eliminate the error due to inaccurate setting of the sensor.

When the values of the acceleration to be measured are large, i.e., when  $a \gg \epsilon$ ,

$$P \approx ma \left( \cos \alpha + \frac{\epsilon}{a} \sin \alpha \right).$$

and the error due to the inaccurate setting will be

$$\frac{\Delta a}{a} = 1 - \left( \cos \alpha + \frac{\epsilon}{a} \sin \alpha \right).$$

It is apparent that the error will decrease with an increase in the acceleration to be measured. Values of errors for various accelerations and deviation angles are presented below:

$a$	$\alpha^\circ$	$\Delta a/a, \%$
$g$	5	$\approx 0,3$
$g$	2	$\approx 2,4$
$10g$	5	0,77
$10g$	2	0,25

Sensors used to measure small accelerations should be placed with the greatest feasible accuracy and should operate in a horizontal direction.

If, in the measuring process, the linear acceleration sensors are inclined to both sides at one and the same angle, the null line will not shift, but the greater the amplitude error, the greater will be the angle of deviation of the sensor. If, however, the angles of deviation are different in both directions, a shift will be observed in both the null line and the amplitude error.

The incorrect setting of an accelerometer in the plane of the ac-

celeration to be measured may also give rise to errors.

When the sensor is incorrectly set up, the result is that errors will arise in the amplitude when the direction of the deviation of the mass on the spring does not coincide with the direction of the motion of the body of the sensor. In this case, the amplitude of the recorded acceleration increases in proportion to  $\cos \beta$  where  $\beta$  is the angle between the directions of the deviation and the motion.

An important characteristic of an accelerometer is its ability not to react to accelerations directed at angles to the acceleration to be measured.

This ability depends on the accuracy with which the sensor is built, since it is difficult to exclude slight deviations of the center of gravity of the body of the sensor from its geometrical axes of symmetry. Lateral accelerations create torsion and bending moments which, in their turn, produce bending of the spring of the sensor and can influence the reading of the instrument.

There are many designs of linear acceleration sensors with flat springs of bronze or steel and with small masses in the form of a steel sphere or cylinder.

Sensors can be designed most readily for slow fluctuations, even if for large accelerations. On the other hand, the more rapidly the small-magnitude accelerations change, the more complex will be the designs and the less sensitive the sensors.

The natural vibration frequency of sensors with a single cantilevered beam may be up to 200 - 250 cps. Higher-frequency sensors manifest low sensitivities.

The upper limit of an acceleration to be measured is determined by the bending possible in the sensor spring. Since this value is usually large, the upper limit of accelerations which can be measured

will also be high.

For example, a sensor with a natural frequency of 59 cps at an acceleration of 1 g produced an oscillograph-beam deflection of 24 mm. To this acceleration corresponded a spring deflection of 0.1 mm. The largest spring deflection at which the greatest stress did not, by far, reach the proportion limit was 2 mm. Therefore, the sensor can measure an acceleration of the order of  $\pm 20$  g. In this case, the magnitude of the acceleration to be measured is now limited not by the sensor, but by the loop of the oscillograph. Since, at an acceleration of 1 g, the current at the output of the amplifier is 1.25 milliamps, we may measure an acceleration not greater than 4 g with the loop selected (class V with a maximum current of 5 milliamps), and the limits of the sensor measurements will be from 0.25 to 4 g. Taking a loop with different sensitivity (class VI with a maximum current of 25 milliamps), we may, with the use of this same sensor, measure accelerations in the range of  $\pm 20$  g with a sensitivity of 5 mm/g.

A natural frequency of a sensor of 200 cps which permits measurement of the harmonic fluctuations of an acceleration with a frequency higher than 70 cps has in many cases proved to be insufficient. To build higher-frequency sensors, it is necessary to search for means of increasing their sensitivity; this may be achieved by several methods. The first method consists in the use of strain-gage pickups made of materials with large deformation effects: Chromel ( $\gamma = 2.8$ ), Elinvar ( $\gamma = 3.6$ ), and a five percent platinum-iridium wire ( $\gamma = 5.1$ ). The second method consists in design improvements and an increase in the number of operating strain-gage pickups; the third consists in using unglued wire-wound resistors.

The first method is the simplest, but requires a special wire which is not always on hand.

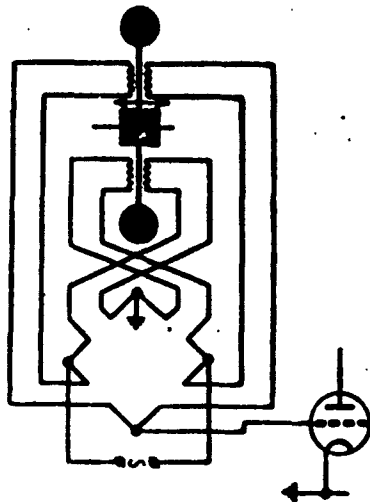


Fig. 31. Sensor with increased sensitivity.

The second method is also not complicated and may be used by changing the design of the acceleration sensor. In this sensor, there are two similar cantilever beams, one end of each of which is fastened to a single support. The weights fastened at the free ends also have equal masses. Wire-wound resistors are fastened on the two beams and are connected to one bridge in such a manner that when the beams bend to one side, the bridge acquires a maximum imbalance (Fig. 31). The damping

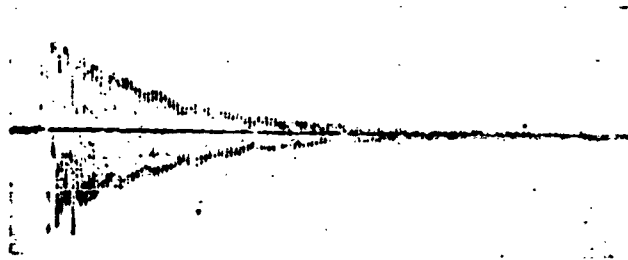


Fig. 32. Damping vibrations of sensor with two beams.

vibrations of this sensor which are excited, for example, by an impact on the casing, will have pulsations (Fig. 32) which are caused by the different natural frequency of the beams. Damping the sensor will free it of the natural frequency vibrations but in measuring, the pulsations may introduce amplitude errors; therefore, these must be eliminated by prolonging the beat-frequency period. This effect can be achieved by selecting the lengths and masses of the weights so that their vibration frequencies coincide or become very close.

To increase the sensitivity, we may use designs in which the de-

formation of the strain-gage pickups is increased. In these designs (Fig. 33), the wire-wound strain-gage pickups are glued not on the spring bearing the weight, but on thin strips of brass or bronze foil connecting the weight with the base of the sensor and forming a rigid closed triangle. The inertial force of the mass of the weight will elongate one strip and compress the other. In order that the strips cannot be unloaded on compression, they should be pretensioned; this is guaranteed by a corresponding device in the sensor design. The same device is used to eliminate the pulsations.

One similar design had a natural frequency of 1450 cps and a sensitivity approximating that of a sensor with a natural frequency of about 50 cps.

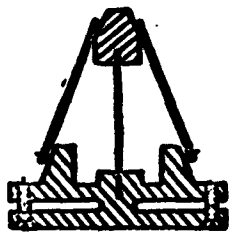


Fig. 33. Diagram of high-frequency sensor.

An even greater degree of sensitivity may be obtained in the design described above which consists of installing unglued wire-wound resistors in place of the foil strips. In this case, the wire of the strain-gage pickup is wound directly on a manifold on the weight and the base. In this design, the sensitivity is increased at the expense of greater wire deformation. In addition, a

heavier-gage wire (with a diameter from 0.05 to 0.06 mm) may be used for the winding; this permits an increase in the feed voltage to the measuring bridge.

A disadvantage of the unglued wire-wound resistors is their high sensitivity to the slightest vibrations of the air, which cause unstable readings on the recording instrument and make it difficult to balance the bridge. This makes the sensor useful only in cases where the entire system is placed in a damping liquid. In this case, the readings of the instrument are completely stabilized. A further dis-

advantage of these sensors is their low strength and the possibility of breaking the wire on dropping, shock, etc.

This drawback is avoided by introducing into the design an arresting device which backs up the elastic system of the sensor.

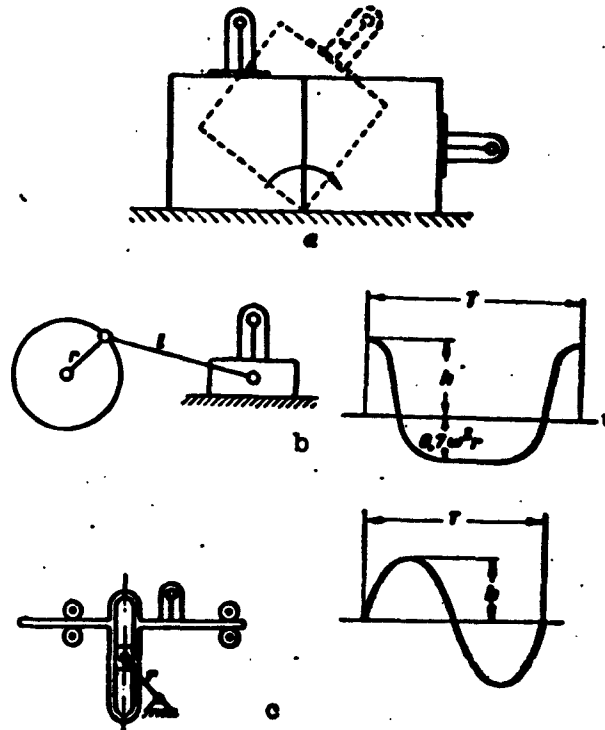


Fig. 34. Calibration of linear acceleration sensors.

It is best to calibrate the sensor before each measurement for the measurement of small linear accelerations. To calibrate in the 2 g range, there must be made a metallic cube whose surfaces are rigidly perpendicular to each other.

Placing this cube level so that the upper face is horizontal, a sensor is placed on it and its null reading is noted. Turning the cube about the face perpendicular to the vibration plane of the sensor in both directions, we obtain  $90^\circ$  inclinations of the sensor and a reading that corresponds to 1 g (Fig. 34a).

Thus, we may calibrate sensors with high sensitivity which are intended for the measurement of small accelerations. For high-frequency sensors with low sensitivities, the deviation of the light indicator of the oscillograph, which corresponds to 1 g, will be small, and when employing the indicator, significant errors may be present.

It is better to calibrate the high-frequency sensors on special installations. This equipment may be, for example, a rotating horizontal disk or bar at the end of which is placed a sensor connected to the measuring instrument by contact rings. Knowing the distance  $r$  from the center of rotation to the center of gravity weight of the sensor, and measuring simultaneously the angular velocity of the rotating disk, by sensor readings, we can determine the acceleration from the formula

$$a = \omega^2 r.$$

The value of such a calibration is the possibility of attaining extremely large accelerations. The disadvantage, however, is the necessity of having a current pickup, as well as the considerable dimensions of the pickup itself. It is also necessary to provide a smooth and even rotation of the apparatus. This method may be used to calibrate sensors that permit the use of static calibration.

The calibration of linear acceleration sensors may also be accomplished by the use of a mechanism of which one linkage has a reciprocating motion. Such a mechanism is, for example, a crankgear.

Figure 34b shows a curve for the dependence of the acceleration of a central crankgear slidebar with a ratio of  $r/l = 0.3$  on the deflection angle of the crank. On the portion corresponding to the deflection angle of the crank from  $140^\circ$  to  $220^\circ$ , the acceleration of the slidebar is constant and is  $0.7 \omega^2 r$ . This rectilinear portion of the acceleration curve may be used to calibrate sensors. The acceleration

of the slidebar is  $1.3 \omega^2 r$  at the point which corresponds to the zero position of the crank.

This point may also be utilized for low-speed calibration. For high-speed calibration, the ordinate of the peak is read with less accuracy; consequently, it is considerably more convenient to use the rectilinear portion of the curve in the case in question. Thus, the slidebar of the crankgear with a ratio of the crank radius to the connecting rod of  $r/l = 0.3$  may be employed to calibrate sensors used to measure linear accelerations. Knowing  $r$  and determining  $T$  from the oscillogram, we find the magnitude of the acceleration

$$a_1 = 0.7 \cdot \frac{4\pi^2}{T^2} r$$

and the maximum acceleration

$$a_2 = 1.3 \cdot \frac{4\pi^2}{T^2} r.$$

this acceleration corresponds to the zero position of the crank.

Dividing the acceleration thus obtained by the ordinate (in millimeters), we obtain the measurement scale

$$k_a = \frac{a_1}{h_1} = \frac{a_2}{h_2} \frac{\text{m/sec}^2}{\text{mm}}$$

Figure 35 shows an oscillogram of the displacement, velocity and acceleration of a crankgear slidebar with a ratio  $r/l = 0.3$ , from which it is apparent that the rectilinear portion of the acceleration curve may be readily measured.

For calibration, the "sine" mechanism may be used (Fig. 34c); in this case

$$a = \frac{4\pi^2}{T^2} r.$$

Where the dimensions of the mechanism are large and the velocities high, we may obtain large accelerations but, in this case, difficulties are created due to the friction of the slidebar and the clearances at the joints. The choice of clearances produces peaks on the

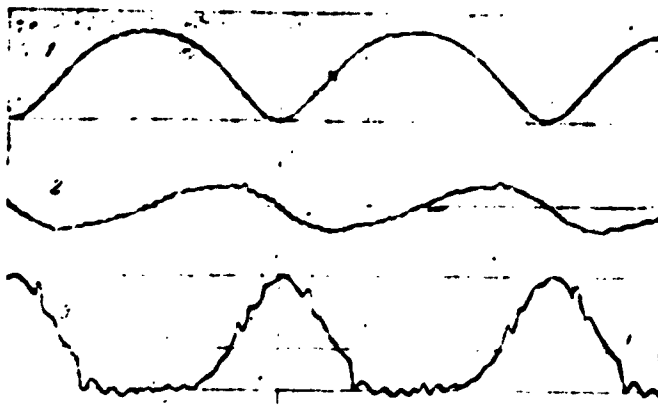


Fig. 35. Oscillogram of crankgear slide-bar parameters. 1) Displacement; 2) velocity; 3) acceleration.

acceleration curve, while the friction gives rise to unstable, non-periodic vibrations which decrease the accuracy of the reading. By decreasing the friction of the slidebar, we may improve the conditions and the accuracy of the sensor calibrations considerably. Calibrations of instruments with crankgears or sine mechanisms are convenient because the amplitudes of the vibrations in them have constant magnitudes. The values of the acceleration and the sensor scale are read directly from the oscillogram. The disadvantages mentioned, however, limit the application of these mechanisms to accelerations of not more than 15 to 20 g at frequencies in the neighborhood of 50 cps.

Vibrating tables may also be used for calibration. The presence of gears, joints, and sliding couples in their designs, however, superimposes on the basic acceleration curve unstable vibrations that make analysis of the oscillogram difficult. We can obtain a higher frequency on vibrotables than on mechanical equipment, but they still generally require measurement of the vibration amplitudes; this sometimes causes difficulty when the amplitudes are small. Only vibrators with elastic components produce smooth acceleration curves.

In installations in which the sensor apparatus was on a cantilever beam in which natural vibrations were excited, the acceleration oscillogram of these vibrations had a smooth form. Since, in this case, backlashes and friction were absent, the accelerations obtained were without distortions. The cantilever beam may be used to calibrate linear acceleration sensors.

If a wire-wound strain-gage pickup which measures the beam deflection or vibration amplitudes is glued to a beam, we may determine the magnitude of the maximum acceleration of the vibrations of the beam. For this purpose, it is necessary to record the deflection of the beam and the vibration accelerations simultaneously and to determine the amplitude corresponding to the selected vibration. Since the beam performs harmonic vibrations, the maximum ordinate of the acceleration curve on the oscillogram, which corresponds to the given vibration, will express the linear acceleration

$$a_{\max} = h_0 \omega^2,$$

where  $\omega$  is the angular frequency of the vibrations of the beam and  $h_0$  is the beam deflection that corresponds to the given amplitude of the acceleration.

The vibration period  $T$  is determined on the same oscillogram from the time marker.

It is better to excite vibrations in the cantilever beam not with an electric motor with imbalances, but with a small pneumatic turbine with an unbalanced load, since the sparking on the commutator of an electric motor situated near the sensor greatly alters the reading. A pneumatic turbine will not create such disturbances. The available cantilever beams with pneumatic excitation made it possible to obtain a vibration frequency up to 100 cps at a maximum acceleration from 25 to 30 g.

Electromagnetic vibrating tables are widely used to calibrate and to record the characteristics of vibrometers and accelerometers. There are very many designs for these tables [7]. Their characteristic property is the possibility of obtaining harmonic vibrations over a wide frequency range and in an accurate form. There are tables which enable us to obtain vibrations with frequencies up to 10 kcps. The table vibrations are excited by a sound generator which feeds the windings of a coil which vibrates in the field of a stationary magnet. The frequency of the vibrations is readily determined from the generator dial or from the oscillographic reading. Vibration amplitudes of the order of 0.1 mm can be measured successfully from blurring of the image of a glued, fine (0.03 mm), bare wire with the aid of a gaging microscope. At higher frequencies, the amplitudes of the table vibrations become negligibly small and can be measured by means of an interferometer. The technique of such measurements is complex and cannot always be used in laboratory practice. Using the amplitude measurements from the first method, we can obtain accelerations of the order of from 200 to 300 g at a frequency from 2 to 3 kcps on similar tables.

#### 7. MEASUREMENT OF IMPACT ACCELERATIONS

Impact accelerations are specific. The curves of the impact parameters have unique and well-defined forms of fluctuations which occur in ten and one-hundred thousandths of a second. The measurement and recording of such processes require special sensors, amplifiers, and recording instruments.

The sensors should have a high natural frequency, the amplifiers a wide transmission band, and the recording apparatus should be without inertia and adapted to record curves of the type indicated above.

A sensor which measures impact accelerations is an essential part of the apparatus and the greatest attention must be paid to it because

it differs essentially from the sensors described earlier.

With its apparent simplicity, the impact process turns out to be complex. On impact, vibrations arise in the colliding components; repeated impacts with smaller accelerations occur. All these vibrations and impacts excite vibrations in the connected components which are transmitted to the measuring instrument and excite resonant vibrations of various harmonics in it. As a result, an oscillogram is obtained with complex vibrations of different frequencies between which it is difficult to distinguish.

Figure 36 shows the impact of a rod falling vertically onto a steel plate, which is recorded by the contact method with a cathode-ray oscillograph. On contact of the rod with the plate, an electric circuit is closed and the beam is deflected toward the vertical.



Fig. 36. Impact recorded by contact method.

After one fall of the rod, several collisions result which are recorded as straight lines, the time between which becomes shorter with each collision as the time of the collision increases.

If we record the movements of this rod (Fig. 37) during its fall and the impact accelerations, an oscillogram is obtained on which the rebounds and decreasing magnitude of acceleration are clearly visible.

The impact accelerometers intended for measurement of very short-time accelerations are instruments with inertial elements.

The mechanical characteristics of an impact acceleration sensor should correspond to the impact characteristics; this refers primarily to the natural frequency of the sensor.

In order to solve the problem relating to the required natural frequency of the sensor, we must consider and determine the parameters

of the impact itself and, in particular, the duration of the collision.

The problem of collision duration has been examined in literature many times. One of the later studies in this field has been the work of B.M. Malyshev which was printed in the Herald of the Moscow University, No. 5 (1952). In connection with the problem under consideration, of verifying the correctness of calculations made by the hypotheses of Saint Venant, Hertz, and others, an apparatus was constructed which was capable of counting one one-hundred thousandths of a second, with the aid of a generator and an electronic counter.

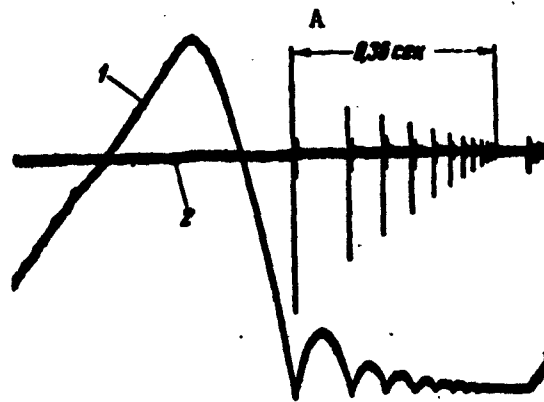


Fig. 37. Displacement and acceleration of falling rod on impact. 1) Displacement of rod; 2) recording of acceleration sensor. A) 0.36 second.

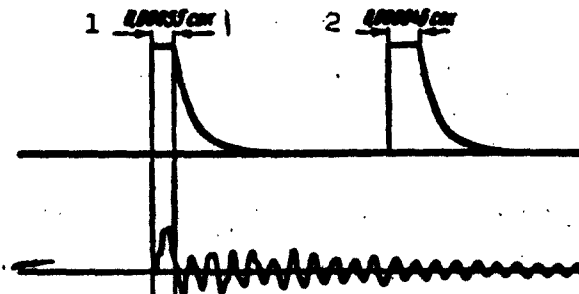


Fig. 38. Oscillogram of collision duration. 1) 0.00055 second; 2) 0.000645 second.

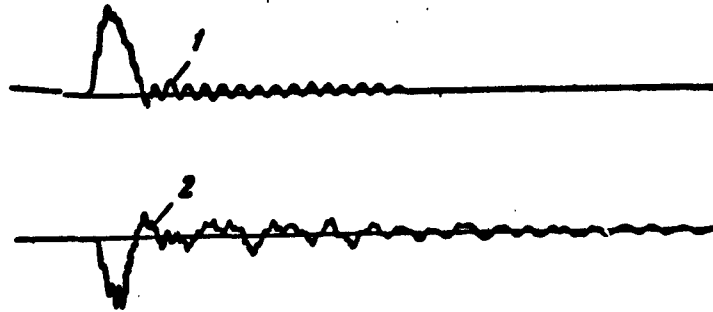


Fig. 39. Deformation (1) and acceleration (2) curves on impact.

The collision time was determined for steel rods and spheres. The durations of the rod collisions were determined in the range from 600 to 780 microseconds as a function of the rod lengths. The sphere impacts were considerably shorter with respect to time and were in the range from 20 to 160 microseconds at collision velocities of from 60 to 0.9 m/sec.

To convert the values for collision durations to accelerometer frequencies, it was also necessary to determine the form of the acceleration change on impact.

To solve these problems, several experimental installations were built. The first was a rod with an accelerometer located on it. The rod was raised by a cam to a height of 5 cm and fell freely onto a doubly-supported removable beam of varying rigidity.

The problem of collision time was solved by the contact method mentioned above. To measure the time of the first contact, it was necessary to increase the velocity of the paper on which the impact was recorded to 30 m/sec with a simultaneous recording of the time. The oscillogram obtained in this case had the form shown in Fig. 38.

The duration of certain types of collision is given below in seconds.

Two steel spheres . . . . .	0.00022
Rod and steel plate . . . . .	0.00037
Rod and most rigid beam . . . . .	0.00046
Rod and least rigid beam . . . . .	0.00079
Rod and non-rigid beam . . . . .	0.00147

The collision time, as is known, is the sum of the time of deformation increase on impact and the time of the deformation decrease. Generally speaking, the time of increase and the time of decrease are unequal, and the time of increase is usually somewhat shorter than the time of decrease, although this is dependent to a considerable degree upon the conditions of the experiment and the rigidity of the colliding bodies. To resolve the question of the required frequency of the sensor to measure accelerations, it may be assumed that the time of increase is equal to one-half the contact time and that the increase and decrease curve can be represented by a portion of a sine curve. Fig. 39 describes the beam deformation and acceleration curves obtained on impact which confirm this characteristic of the curves. Much information may be gotten from these curves. On this basis, we can assume that the contact time on impact is determined to be one-half the period of the sinusoidal process. The period of the natural vibrations of a sensor used to measure accelerations, keeping in mind the difficulty of damping a sensor, should be shorter by at least a factor of ten. On the basis of the measurements and assumptions made, it is possible to confirm that to measure the shortest impact acceleration, it is necessary to have a sensor with a frequency not lower than 25 kcps.

Thus, for the measurement cases cited above, it is necessary to have acceleration sensors with the following natural frequencies:

1 Продолжительность контакта, сек	2 Собственная частота датчика, кц (не ниже)
0,00020	15000
0,00030	10000
0,00045	7000
0,00075	4000
0,00125	2500

1) Contact duration, sec; 2) natural frequency of sensor, cps (not lower).

one-half the collision time,

$$a = \frac{hv}{0.5t}$$

In our case, the height of the fall of the rod was 5 cm. The velocity at the end of this path  $v = \sqrt{2gH}$  is ~1 m/sec. Therefore, the acceleration of an impact on a beam, which has a duration  $t_u = 0.0008$  sec, is ~250 g.

Of course, this method is inaccurate, since an error of only 0.0001 second in the measurement of the collision time will produce a difference of 20 g in the acceleration, i. e., 8%.

#### 8. SENSORS FOR MEASUREMENT OF IMPACT ACCELERATION

If the impact characteristics and requirements of the impact acceleration sensors are known, the problem of fabricating these sensors reduces to a search for designs which have sufficient elasticity, high natural frequency, and simple form, and which would guarantee the absence of the vibrations which accompany the fundamental vibrations.

Figure 40 shows several impact acceleration sensors which were built and tested. They all use wire-wound strain-gage pickups as the sensitive elements. Although the designs in schemes 1 and 2 were sufficiently sensitive, on impact, the vibrations of the stands, casings, and bases of the sensors introduced many additional vibrations which

The data on collision duration can be used to determine an acceleration under the condition that the magnitude of the velocity at the moment of collision is known.

If we assume that the velocity of a colliding body goes from a maximum value to zero over a period of

greatly contaminated the fundamental vibrations; these designs were rejected for this reason. The sensors in schemes 3 and 4 are designs

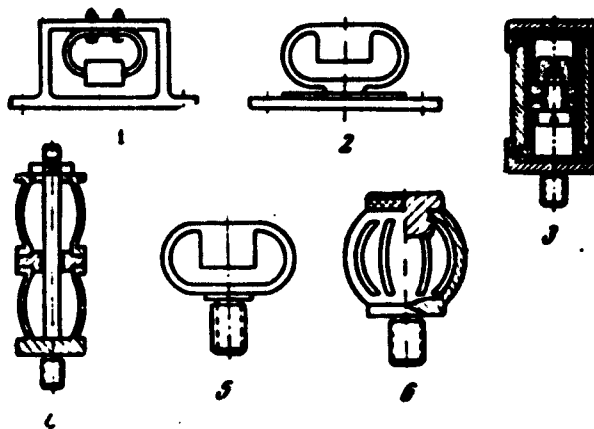


Fig. 40. Impact acceleration sensors with wire-wound resistors.

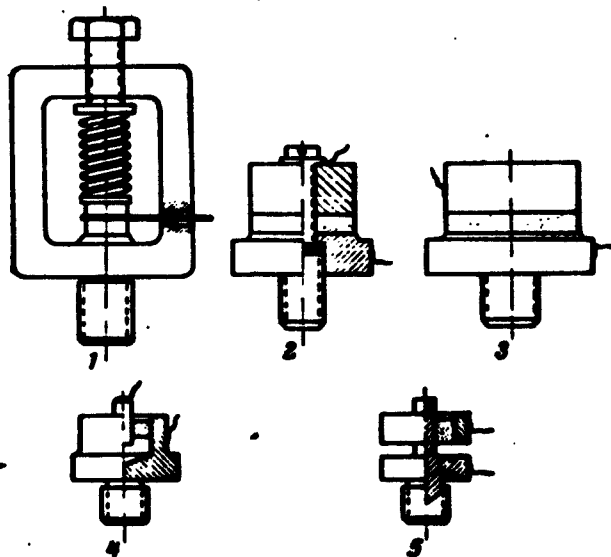


Fig. 41. Diagrams of piezoceramic sensors.

in which the sensitive elastic member is pretensioned (3) or precompressed (4).

The sensor with the pretensioned system has a natural frequency of 17,000 cps and is sufficiently sensitive. The sensor under initial compression is more simple to adjust, but is awkward to use.

Where the natural frequencies are of the same order, the sensitivity of the precompressed sensor is higher than that of the pretensioned sensor.

The two last sensors are the most highly perfected. The first (5) is a steel or bronze oval with a weight in the center portion which is attached to the component by means of a screw. The entire sensor is made of one piece of metal. Wire-wound strain-gage pickups which measure deformations on impact are glued on the internal and external lateral surfaces. The natural frequency of the sensor can vary as a function of the dimensions of the oval and the weight. For sensors made from steel in the machine dynamics laboratory, the natural frequency was 3150 cps. By increasing the dimensions of the oval, the natural frequency may be increased from 4 to 5 kcps. Sensors of larger dimensions with higher natural frequencies have low sensitivities.

The last (6) is a higher-frequency sensor; it is also made of one piece of steel or bronze and has a barrel-shaped form. The lateral surface is divided into an equal number of sections by side-to-side notches. Strain-gage pickups are glued on the inside and outside of all or half of these sections, forming one-half of the measuring bridge. A sensor was attached to the member with a screw. A variable weight was screwed into the top section of the barrel-shaped body.

For the bronze sensor with an outside diameter of 45 mm and a height of 40 mm with a 150 g weight, the natural frequency was approximately 10 kcps. The more severe impacts are measured with this sensor.

In order to obtain impact acceleration sensors with higher natural frequencies, piezoceramics made of barium titanate must be used instead of wire-wound strain-gage pickups as the sensitive elements in the sensors. Since they have a high sensitivity, piezoceramics are now

widely used in measuring techniques.

Ceramics made of polycrystal barium titanate [23] are produced by pressing, firing, and polarization in a high-voltage field. Like other piezoelectric materials, the magnitude of the charge arising on the surface of the piezoceramic is proportional to the applied pressure. Ceramic is rigid and can be loaded to  $800 \text{ kg/cm}^2$  with the deformation of 0.0001%. Due to the brittleness of ceramic, the accuracy requirements of the surfaces which bear on the ceramic surfaces are strict, because the appearance of local pressures may lead to breaking of the piezoelement. The piezoelectric constant of barium titanate ceramic (equal to  $2.5 \cdot 10^{-6}$ ) is less than that of Rochelle salt, but is considerably greater than that of quartz.

The sensitivity of ceramic changes with changing temperature by approximately 0.15% for each degree, and at temperatures of  $-50^\circ\text{C}$  and  $+100^\circ\text{C}$ , the polarization disappears. The humidity also strongly influences the sensitivity.

Piezoceramic sensors are used mainly where short-time pressures and accelerations are to be measured.

Figure 41 shows several designs of sensors used to measure maximum impact accelerations.

The first sensor employs two ceramic disks each with a diameter of 10 mm and a thickness of 4 mm. A contact plate made of thin brass foil with a well insulated output is placed between the two disks. Sometimes this plate is interchanged with a metal disk of approximately the same dimensions as the ceramic disks. In these cases, the plate plays the role of the inertial element. The weight is more frequently superimposed as in the case shown on the diagram. A necessary element in this design is an elastic element in the form of a spring, membrane or other material, which compresses the ceramic and the

weight. The depressing force of the spring must be greater than the inertial force of the weight on impact. If this is not true, at the moment of impact, the weight may separate from the ceramic and alter the reading.

The connection of the sensor to a component must be rigid and should not permit any change on impact.

A sensor made on the basis of this scheme had a high natural frequency (more than 20 kcps) and a high sensitivity (approximately 20 millivolts/g), but the presence of the casing, spring and other components introduced many additional vibrations into the recording and complicated the recording on the oscillogram.

In scheme 2, the ceramic element was made in the form of a collar with a diameter of 25 mm, a thickness of 2.5 mm, and a center opening of 5 mm. A weight attached by an insulated screw was located on the collar. In this case, the absence of a casing produced a smoother recording on the oscillogram.

The sensor of scheme 3 is distinguished from the preceding sensors by the fact that here, the weight and the ceramic are glued to the base. Such bracing simplifies the design and decreases the demands for machining of the base and weight surfaces that come in contact with the ceramic. Since the strength of the glue may be found inadequate under large accelerations, the dimensions of the ceramic and the weight of glued sensors are made as small as possible.

One of the principal drawbacks of ceramic sensors is their lateral sensitivity to action in the plane perpendicular to the direction of measurement; this can amount to 20-25%.

In the foreign literature and in the studies of several of our institutes and laboratories (for example, TsNIITMASH [Central Scientific and Research Institute of Technology and Machine Construction]),

sensor designs may be found in which the lateral sensitivity is eliminated by the fact that the take-off of the charges arising on the ceramic when it is under pressure is not accomplished from the front surfaces, as is usually done, but from the side surfaces. In making these sensors, the ceramic is polarized in the usual manner, but it is not the front surfaces, but the sides from which the charges are taken off which are coated with silver. Sensors made on the basis of this scheme (4 and 5 in Fig. 41) were tested simultaneously with other types of sensors, and their lateral sensitivity was measured. The tests were conducted on a cantilever beam, the vibrations of which were excited by a vibrator (a small direct-current motor with unbalanced disks). The tests were conducted at one frequency, equal to 100 cps. A sensor was arranged on a rotating device which enabled us to turn the sensor through an angle to the direction of the vibration of the beam. The vibration amplitude was measured on the screen of a loop oscillograph after each  $30^{\circ}$  rotation. The results of the measurements for the sensors in scheme 2 shown in Fig. 41 are arranged in the form of a polar diagram (Fig. 42).

For sensors on which the charge is taken off from the lateral surface, the lateral sensitivity is decreased almost half, and occasionally even more. The sensitivity of these sensors in a straight line is not less than that of ordinary sensors.

The accelerations on impact exceed those of the nonimpact processes by tens of times.

It is extremely complicated to obtain an accurate value for a large acceleration under laboratory conditions. Thus, for an acceleration of 1000 g, it is necessary to cause a calibrated table to vibrate with a frequency of 160 cps and an amplitude of 10 mm. At first glance, realization of such conditions seems uncomplicated; however,

in order to carry this out, we are required to use a great deal of power; this involves use of a power plant, building a substantial foundation, rigid bracing, etc.

Under ordinary laboratory conditions, considerable accelerations were obtained on several installations. The first of these was a cantilever beam with a length of approximately 300 mm, a width of 60 mm, and a thickness of 6 mm. Wire-wound strain-gage pickups were glued on the beam around the rigidly secured end in order to measure the deflection of the beam. Calibration of the deflection was carried out statically by a screw and a time indicator.

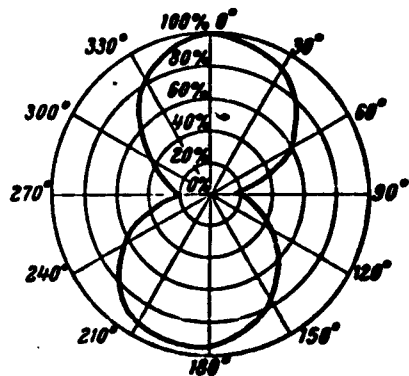


Fig. 42. Sensitivity of piezoceramic sensor to acceleration directed at an angle.

the amplitude for each vibration and calculate the frequencies of the vibrations. The maximum acceleration value which refers to the corresponding amplitude of an acceleration is determined from these values. The acceleration scale will be

$$k_a = \frac{4\pi^2}{T^2} \cdot \frac{r}{A} \cdot \frac{\text{m/sec}^2}{\text{mm}}$$

where  $r$  is the amplitude (deflection) of the beam, meters,  $T$  is the period of one vibration, sec;  $A$  is the ordinate of the maximum acceleration, mm. We can obtain accelerations with magnitudes of 150 g on

this apparatus.

The second apparatus is analogous to the first, but with not one but two beams connected together and having a resemblance to a tuning fork being employed. Beams with dimensions of 480 X 100 X 12 mm took the form of a beam of equal resistance. Such a design permits dissipation of the vibration energy within the apparatus and does not permit transmission of it to the support; this was observed in the former design and gave rise to vibrations of the floor. The form of a beam of equal resistance was selected to decrease the wedge-displacement force which transmits vibrations to the beams and to increase the natural frequency. A calibrated sensor was placed on the end of one beam and a weight equal to the weight of the sensor was set on the other end. In this case, a curve of the damping vibrations was obtained without pulsations. On this apparatus, it was possible to obtain accelerations up to 500 g. On it, the calibrations of the piezoceramic acceleration sensors were carried out at a frequency of approximately 150 cps. In tracing on an electronic oscillograph, it is impossible to make a static calibration of a beam deflection even though we are restricted only by the value of the deflection obtained when the wedge is pulled out.

These disadvantages limit the application of the apparatus to the calibration of sensors used to measure comparatively slowly-increasing accelerations which may be recorded on a loop oscillograph. To calibrate the sensors used to measure sudden impact accelerations, it is necessary to use another type of apparatus, for example, one with a ballistic pendulum.

#### 9. CALIBRATION OF IMPACT ACCELEROMETERS

The calibration of accelerometers used to measure impact accelerations may be carried out, like the calibration of "ordinary" accel-

erometers, under conditions of forced harmonic vibrations, on a vibrostand. The vibrostand must create vibrations of the proper form and of sufficiently large amplitude at frequencies of at least 4 to 6 kcps, to make it possible to attain acceleration of several hundred  $\underline{g}$  and more. As yet, there are but a few similar stands; therefore, as a substitute (although not quite the equivalent), we propose calibration by the use of a ballistic pendulum.

The ballistic pendulum has been described in the literature [20] and [41]. Its working principle is evident from Fig. 43.

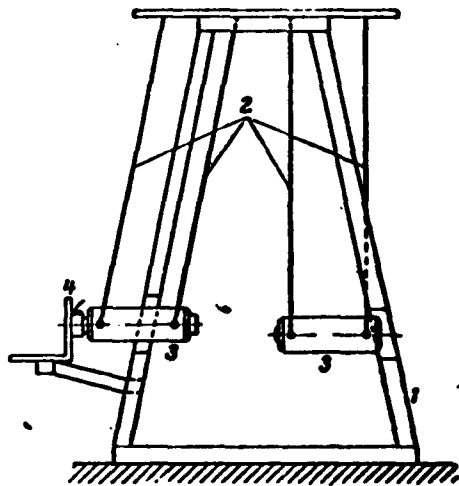


Fig. 43. Simplified diagram of ballistic pendulum. 1) Frame; 2) threads; 3) weights; 4) electromagnet.

The frame on which the pendulum is erected is made of steel angle brackets in the form of a truncated tetrahedral pyramid with a height of approximately 1 m. The weights are metallic cylinders with a diameter of 70 mm and a length of 250 mm, each of which is suspended by eight threads so that their movement takes place as far as possible in one plane. The masses of the weights are equal. The collid-

ing surfaces are made of tempered steel. In the rear portion of the colliding weight is a steel insert by which the weight may be restrained by an electromagnet. The electromagnet may be shifted, thus varying the velocity of the colliding weight. In calibration, it is necessary to know the velocity of the colliding weight  $v_0$  and to record the acceleration curve as a function of time. Obviously, it is necessary first to determine the natural frequency of the accelerometer and to evaluate the collision time in order to be solidly con-

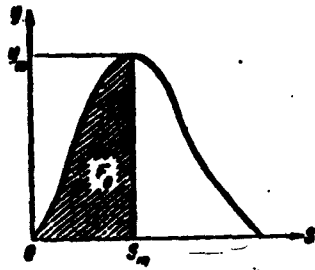


Fig. 44. Determination of acceleration scale on impulse oscillogram.

vinced of the accuracy of the accelerometer readings.

The determination of the acceleration scale and magnitude of acceleration is illustrated in Fig. 44 which represents a portion of an oscillogram obtained.

If we place the scales of the time measurement  $k_t$  and the acceleration measurement  $k_a$  on the oscillogram so that

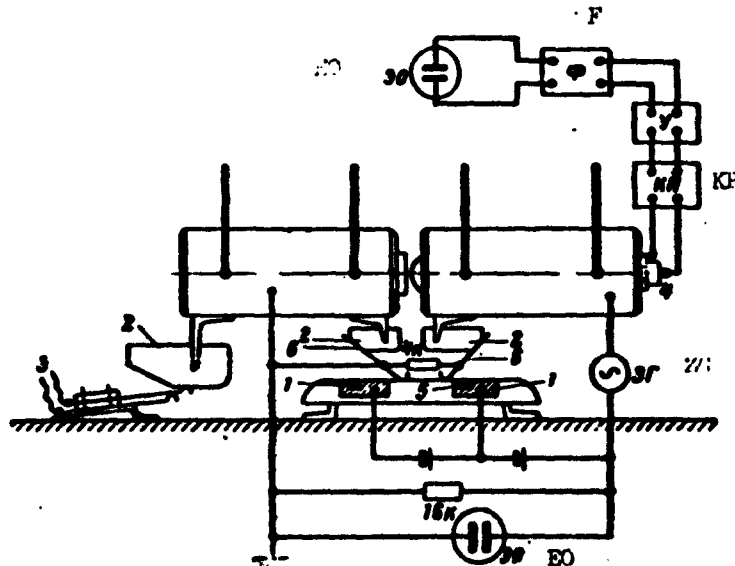


Fig. 45. Detailed diagram of accelerometer calibration by the use of ballistic pendulum. 1) Contact plates for velocity measurement; 2) stand made of insulating material; 3) leads to circuit of oscillograph synchronizer; 4) accelerometer being calibrated; 5) plates made of insulating material; 6) sliding contact. EO) Oscillograph plates; ZG) standard frequency generator; KP) cathode follower; Y) amplifier; F) filter which suppresses standard frequency.

$$t = k_t s; a = k_a y,$$

then obviously

$$v_0 = \int_0^m a \cdot dt = k_a k_t \int_0^m y \cdot ds = k_a k_t F_0$$

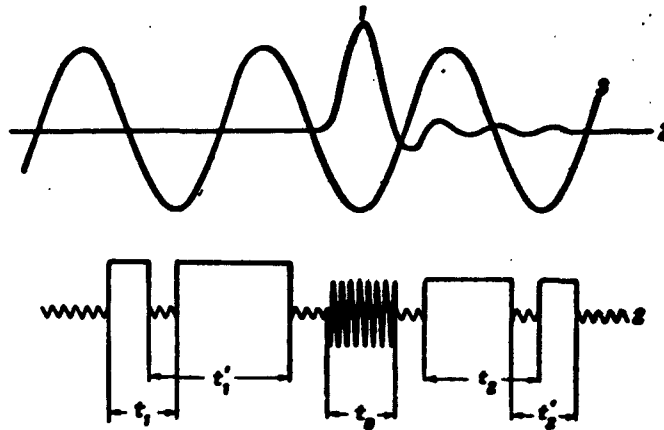


Fig. 46. Example of calibrated oscillogram. 1) Impulse acceleration; 2) record of velocities and collision times; 3) calibration voltage for determination of accelerometer sensitivity.

therefore,

$$k_a = \frac{v_0}{k_t F_0}$$

and the acceleration in impact is  $k_a v_m$ .

When determining  $k_a$ , it is most difficult to calculate  $F_0$ . It is better, of course, to make a graphic integration. If the curve  $y(s)$  is closely similar to a semisinusoid, then  $F_0 = 2s_m y_m / \pi$ . If, however, it suggests the curve  $e^{-\sigma^2 s^2}$ , then  $F_0 = \sqrt{\pi/2\sigma}$ . The principal error of the calibration arises precisely at this stage.

The time scale  $k_t$  is determined by the usual method from the standard frequency. The velocity  $v_0$  is generally calculated from the angle of deviation and the lengths of the threads. But this is not a very accurate and convenient method. The ballistic pendulum of the ma-

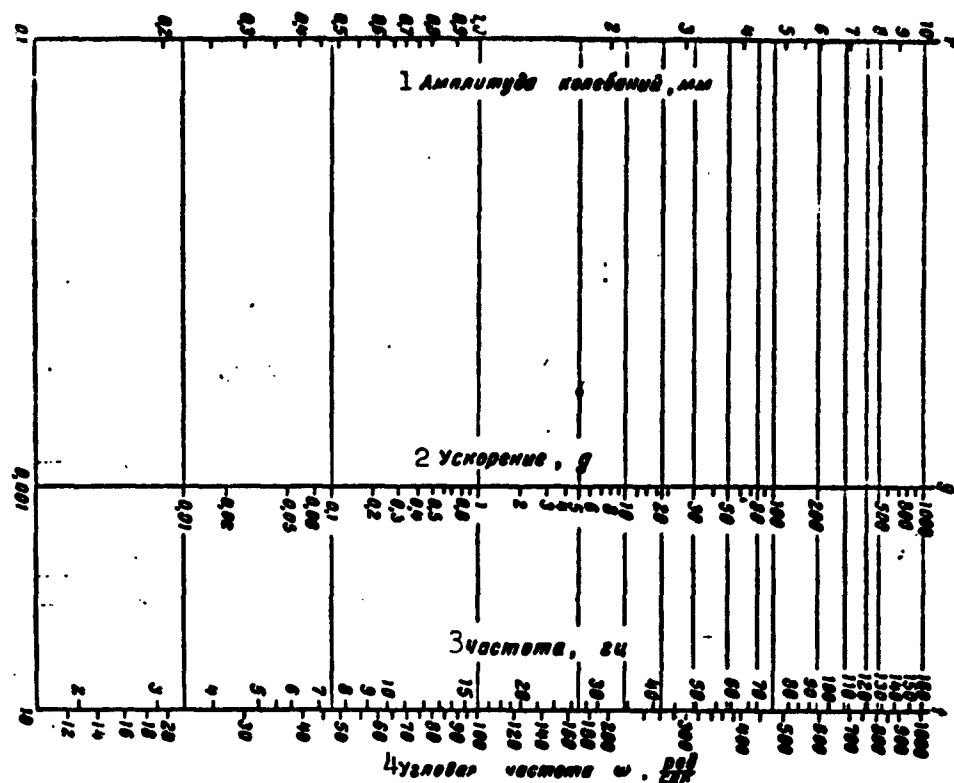


Fig. 47. Nomogram for determination of acceleration of harmonic vibratory motion. 1) Amplitude of vibrations, mm; 2) acceleration, g; 3) frequency, cps; 4) angular frequency  $\omega$ , radians/sec.

chine dynamics laboratory was provided with a simple arrangement for recording the time and the velocity  $v_0$ , as well as the velocity of the second weight on the screen of a double-beam oscillograph. This arrangement is depicted schematically in Fig. 45, and the oscillogram obtained is shown in Fig. 46 (for convenience of description, the time scale is condensed at the individual points).

In the arrangement for velocity determination, the contact plates each consist of two parts so that variations in the dimensions of a movable contact do not show in the results. In reading, the time is taken from the first to the second circuit closings ( $t_1$  and  $t_2$ ) or from the first and second openings ( $t'_1$  and  $t'_2$ ). The corresponding

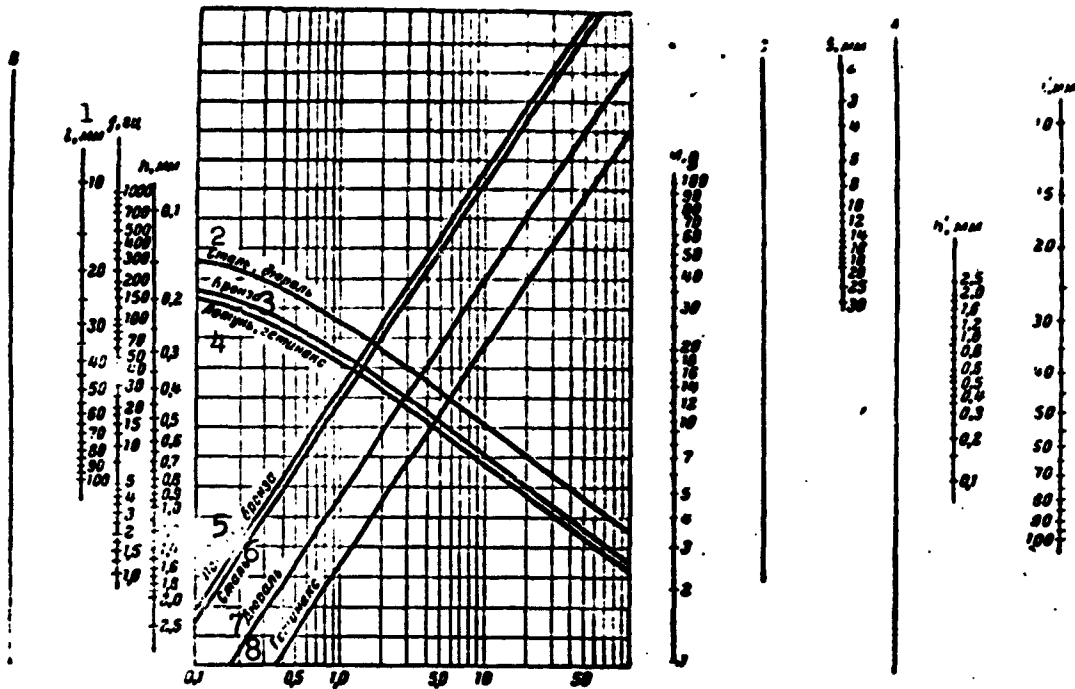


Fig. 48. Nomogram for design of accelerometers. 1)  $f$ , cps; 2) steel, Dural; 3) bronze; 4) brass, Micarta; 5) brass, bronze; 6) steel; 7) Dural; 8) Micarta.

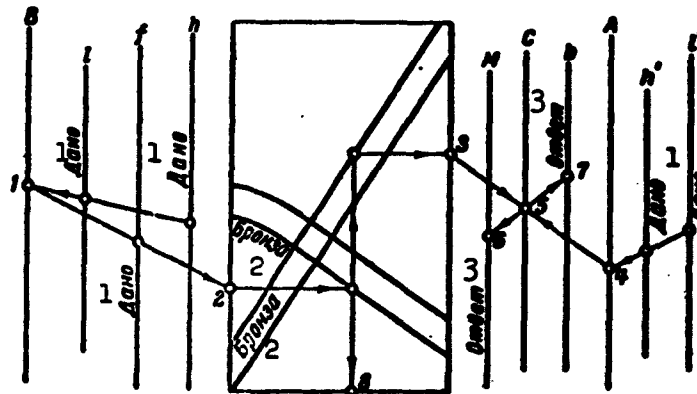


Fig. 49. Diagram of use of nomogram shown in Fig. 48. 1) Given; 2) bronze; 3) answer.

intervals on the plates are also measured on the basis of the circuit closings by a movable contact which is shifted with a micrometer screw. A standard frequency generator creates noticeable settings on

the two channels; therefore, a filter in the form of a double T-shaped bridge, which is tuned to this frequency, is connected between the amplifier to the accelerometer and the oscillograph. A small setting on the channel of the velocity and time of impact recordings, however, only aids when the oscillogram is processed. A calibrated voltage of lower frequency, which is supplied to the amplifier to determine the voltage sensitivity of the accelerometer (millivolt/g), is also apparent on the oscillogram.

Manu-  
script  
Page  
No.

[Footnote]

- 1 The most general designation for an instrument used to measure accelerations.

Manu-  
script  
Page  
No.

[List of Transliterated Symbols]

- 10 BMX = vykh = vykhod = output  
14 y = u = uprugiy = elastic  
14 c = s = sila = force  
36 II = D = Datchik = Sensor  
54 y = u = udaryayushchiy = colliding

#### REFERENCES

1. Anan'yev, I.V., Spravochnik po raschetu sobstvennykh chastot [Handbook on the Calculation of Natural Frequencies], Moscow, 1946.
2. Andrianov, K.A. and Petrenko, A.I., Kremniyorganicheskiye polimery v narodnom khozyaystve [Silicon-Organic Polymers in the National Economy], Moscow, 1959.
3. Arutyunov, V.O., Raschet i konstruirovaniye elektroizmeritel'nykh priborov [Calculation and Physical Designs for Electrical Measurement Instruments], Moscow, 1949.
4. Borkovskiy, R.I., Kats, A.M. and Prokopov, V.K., Teoriya lineynykh fil'truyushchikh akselerometrov [Theory of Linear Filtering Accelerometers], Tr. Leningradskogo politekhnicheskogo in-ta [Transactions of the Leningrad Polytechnic Institute], No. 192, Mashgiz, 1958.
5. Borkunskiy, G.M., Uskoreniye mery s provolochnymi datchikami [Accelerometers with Wire Sensors], Novyye pribory dlya dinamicheskikh ispytaniy vagonov [New Instruments for Dynamic Tests of Cars], Glavnoye upravleniye vagonostroyenoya NIB [Main Administration for Car Building of the Scientific Research Office], Moscow, 1955.
6. Bryuyel', V., Novyye datchiki uskoreniy [New Acceleration Pickups], Collection of abstracts entitled Mashinostroyeniye [Machine Building], 1957, No. 7.
7. Vasil'yeva, R.V., Vibrostendy dlya tarirovaniya vibrometrov i akselerometrov v shirokom diapazone chastot [Vibration Benches for Calibrating Vibrometers and Accelerometers in a Wide Frequency Range], in book entitled Vibroizmeritel'naya apparatura TsNIITMASH [Vibration-Measurement Device of the Central Scientific

Research Institute for Technology and Machinery], Moscow. Mashgiz [State Scientific and Technical Publishing House for Literature on Machinery], 1958.

8. Velev and Geriks, Telemetricheskiy pribor dlya izmereniy uskoreniy i zamedleniy rudnichnykh pod"yemnikov [Telemetric Instrument for Measurement of Accelerations and Decelerations of Mine Elevators], Collection of abstracts entitled Mekhanika [Mechanics], 1954, No. 8.
9. Vershinskiy, S.V. and Fedos'yeva, A.V., Usiliya i uskoreniya, vznikayushchiye pri soydarenii vagonov [Forces and Accelerations that Arise on Coupling of [Railroad] Cars], in book entitled Issledovaniya dinamiki vagonov [Investigation of the Dynamics of Cars], Transzheldorizdat [State Publishing House for Railroad Transportation Literature], 1955.
10. Verkholat, M.Ye., Ustroystvo dlya zapisi skorostey i uskoreniy malykh postupatel'nykh peremeshcheniy [Device for Registering Speeds and Accelerations of Small Progressive Displacements], Stanki i instrumenty [Machines and Tools], 1953, No. 4.
11. Goncharskiy, L.A., Ionnyy datchik uskoreniy [Ionic Acceleration Sensor], Priborostroyeniye [Instrument Building], 1958, No. 2.
12. Den-Hartog, Teoriya kolebaniy [Theory of Vibrations], Moscow, 1942.
13. Zakharov, V.P., Uskoreniyemer s provolochnymi tenzodatchikami [Accelerometer with Wire Strain-Gauge Sensors], in book entitled Izmereniye napryazheniy i usiliy v detalyakh mashin [Measurement of Stresses and Forces in Machine Components], Moscow, 1955.
14. Ivanchenko, G.Ye., Elektricheskiy takhoakselerometr i yego primeneniye v gornoy tekhnike [The Electric Tachoaccelerometer and its Application in Mining Engineering], Ugol' [Coal], 1950, No. 1.
15. Ivanchenko, S., Pribor dlya zapisi uskoreniy sudna pri spuake [Instrument for Recording Accelerations of Ship on Launching],

- Morskoy flot [Maritime Fleet], 1952, No. 11.
16. Iorish, Yu.I., Izmereniye vibratsiy [Measurement of Vibrations], Moscow, 1956.
  17. Kolesnik, P.V., Predel'nyy akselerometr [Maximum Accelerometer]. Vestn. mashinostroyeniya [Herald of Machine Building], 1955, No. 11.
  18. Korepin, Ye.A., K voprosu o raschete kleyenykh p'yezoelektricheskikh preobrazovateley akselerometrov [On the Problem of Designing Cemented Piezoelectric Accelerometer Transducers], in book entitled Nauchno-tekhnicheskaya informatsiya. Byull. Leningradskogo politekhnicheskogo in-ta [Scientific-Technical Information. Bulletin of the Leningrad Polytechnic Institute], 1957, No. 1.
  19. Landau, L.D. and Lifshits, Ye.M., Mekhanika sploshnykh sred [Mechanics of Continuous Media], Moscow, 1954.
  20. Nenyukov, V.P., Zhmur, A.S. and Lyapin, G.L., Primeneniye ballisticheskogo mayatnika dlya graduirovki datchikov uskoreniy [Use of the Ballistic Pendulum to Graduate Acceleration Sensors], Izmeritel'naya tekhnika [Measurement Technique], 1959, No. 2.
  21. Radziyevskiy, B.A., K voprosu o pogreshnostyakh v vibroizmeritel'nykh priborakh [Problem of Errors in Vibration-Measurement Instruments], Dopovidi AN URSR [Proceedings of the Academy of Sciences Ukrainian SSR], 1956, No. 5.
  22. Rayevskiy, N.P., Datchiki mekhanicheskikh parametrov mashin [Sensors for the Mechanical Parameters of Machines], Moscow, 1959.
  23. Rudashevskiy, G.Ye., P'yezokeramicheskiye vibrodatchiki [Piezoceramic Vibration Sensors], ITEIN AN SSSR [Institute of Technical and Economic Information Academy of Sciences USSR], Pribory i stendy [Instruments and Benches], Topic I, P-56-477, Moscow, 1956.

24. Smolyuk, L.A., Akselerometr A-2 [The A-2 Accelerometer]. ITEIN AN SSSR, Pribory i stendy, Topic No. 1. PS-55-489.
25. Strelkov, S.P., Vvedeniye v teoriyu kolebaniy [Introduction to the Theory of Vibrations], Moscow, 1950.
26. Subbotin, M.I., Nomograficheskiy raschet vibroizmeritel'nykh priborov prostogo tipa [Nomographic Design of Simple Vibration Measurement Instruments], Priborostroyeniye [Instrument Building], 1959, No. 6.
27. Subbotin, M.I., Issledovaniye zhidkostnogo demfirovaniya v vibroizmeritel'nykh priborakh [Investigation of Liquid Damping in Vibration Measurement Instruments], Vtoraya nauchno-tekhnicheskaya konferentsiya aspirantov IMASH AN SSSR [Second Scientific-Technical Conference of Graduate Students at the Institute of Machine Construction of the Academy of Sciences USSR], Vol. 1, 1959.
28. Subbotin, M.I., Eksperimental'noye opredeleniye postoyannykh inertsionnykh priborov [Experimental Determination of the Constants of Inertial Instruments], Izv. AN SSSR. OTN [Bulletin of the Academy of Sciences USSR, Division of Technical Sciences], 1958, No. 11.
29. Subbotin, M.I., O chuvstvitel'nosti vibroizmeritel'nykh priborov s tenzodatchikami [Sensitivity of Vibration Measurement Instruments with Strain Gauge Pickups], Izv. AN SSSR, OTN, 1959. No. 4 (Mekhanika i mashinostroyeniye [Mechanics and Machine Building]).
30. Timoshenko, S.P., Teoriya kolebaniy v inzhenerom dele [Theory of Vibrations in Engineering], Moscow, 1959.
31. Ugolkov, F.I., Pribor dlya izmereniya uskoreniy pri ispytani na udarnyye peregruzki [Instrument for Measuring Accelerations in Impact-Overload Testing], ITEIN [Institute of Technical and

- Economic Information], No. PS-55-440, 1955.
32. Fridrikh, G., Elektrodinamicheskiy akselerometr [Electrodynamic Accelerometer], Abstract collection entitled Mashinostroyeniye [Machine Building], 1955, No. 7.
  33. Shchedrovitskiy, S.S., Metody i apparatura dlya graduirovki i proverki akselerometrov [Techniques and Apparatus for Calibrating and Testing Accelerometers], Izmeritel'naya tekhnika. 1958, No. 6.
  34. Elmor, E. and Sends, M., Elektronika v yadernoy fizike [Electronics in Nuclear Physics], Moscow, 1953.
  35. Eriksen, G.U. and Ettl'man, D.D., Malogabaritnyy registriruyushchiy akselerometr dlya izmereniya pri udare [Miniature Registering Accelerometer for Impact Measurements], Mashinostroyeniye za rubezhom [Machine Building Abroad], 1958, No. 12.
  36. Eksin, M.G., Datchik uskoreniy [Acceleration Sensor], Byulleten' izobreteniy [Bulletin of Invention], 1953, No. 1.
  37. Yudin, V.A., Mekhanizmy priborov po izmereniyu i registratsii uskoreniy [Mechanisms of Instruments to Measure and Record Accelerations], in his book entitled Mekhanizmy priborov [Mechanisms of Instruments], Mashgiz, 1952.
  38. Basel, C., Neue Moeglichkeiten in der Bauart von Schwingungsmessgeraeten [New Possibilities in the Design of Oscillation Measuring Instruments], ATM, L. 273 (Oct. 1958), L. 276 (Jan. 1959).
  39. Bremen, J.N. and Nisbet, J.S., Direct Method of Accelerometer Calibration. J. of the Acoust. Soc. of America, January 1958.
  40. Bristow, J.R. and Ellames, F.G., Unbounded Wire Resistance Strain Gauge Accelerometers. J. of Scient. Instrum., 1952, 29, No. 9.
  41. Feder, E.L. and Gillen, A.M., High-Frequency, High-G Calibration. IRE Trans. on Instrumentation, 1957, June.
  42. Giles, C.N., Plastic Blocks Mount Accelerometers. Electronics,

1959, Jan., 32, No. 3.

43. Honnell, P.M., Instrumentation for the Transient Testing of Accelerometers. ISA Proceedings, 7, 1952.
44. Hydrodynamic Development Facilities. Testing Waterbased Craft at Saunders-Roe Ltd. Engineering, 1954, July 23, 178. No. 4617.
45. Kaufman, A.B. and Mitchell, P.R., Microscope Technique for Accelerometer Calibration. Instruments and Automation. September 1955.
46. Levy, S. and Bouche, R.R., Calibration of Vibration Pickups by the Reciprocity Method. J. Res. Nat. Bureau of Standards, 1956, Oct., 57, No. 4.
47. Levy, S. and Kroll, W.D., Response of Accelerometers to Transient Accelerations. J. Res. Nat. Bureau of Standards, 1950, Oct., 45, No. 4.
48. Orlicchio, A.W. and Hieber, G., Trends in Acceleration Measurement. IRE Transactions on Instrumentation, 1957, June.
49. Perls, A., Transient Response of Accelerometers. J. Acoust. Soc. of America, 1953, No. 6.
50. Perls, A., Effect of Spring Mass on Contact Accelerometer Responses. J. Appl. Mech., 1957, June, 24, No. 2.
51. Robert, W., Conrad and Irwin Vigness., Calibration of Accelerometers by Impact Techniques. ISA Proceedings, 1953, 8.
52. Rubin, S., Design of Accelerometers for Transient Measurements. J. Appl. Mech. 1958, Dec. No. 4.
53. Shepard, E.S., Magnetic Springs for Accelerometers. Control Engng, 1957, 4, No. 6.
54. Unholtz, K., The Calibration of Vibration Pickups to 200 cps. ISA Proceedings, 1952, 7.
55. Weiss, D.E., Design and Application of Accelerometers. Proc. Soc. Exper. Stress Analysis, 1947, 4, No. 2.

DISTRIBUTION LIST

DEPARTMENT OF DEFENSE	Nr. Copies	MAJOR AIR COMMANDS	Nr. Copies
		AFSC	
		SCFDD	1
		ASTIA	25
HEADQUARTERS USAF		TDBTL	5
		TDRDP	5
AFCIN-3D2	1	AEDC (AEY)	1
ARL (ARB)	1	AFSWC (SWP)	1
OTHER AGENCIES			
CIA	1		
NSA	6		
DIA	9		
AID	2		
OTS	2		
AEC	2		
PWS	1		
NASA	1		
ARMY	3		
NAVY	3		
RAND	1		
POB	12		
NAFEC	1		
SPECTRUM	1		